

**Volcanology, Petrography, and Geochemistry  
of the Kitselas Volcanic Rocks Compared to  
Rocks of the Telkwa Formation,  
Northwestern British Columbia**

By Nicole T. Boudreau

A Thesis Submitted to Saint Mary's University,  
Halifax, Nova Scotia in Partial Fulfillment of the  
Requirements for the Degree of Bachelor of Sciences, Honours,  
Department of Geology

December 6, 2006

© Nicole T. Boudreau, 2006

Approved: Dr. Jarda Dostal  
Date: December 2, 2006

**British Columbia  
Ministry of Energy, Mines and Petroleum Resources**

**Open File 2007-5**



## Abstract

**Volcanology, Petrography, and Geochemistry of the Kitselas Volcanic Rocks Compared to Rocks of the Telkwa Formation, Northwestern British Columbia.**

By Nicole Therese Boudreau

The Lower Jurassic Kitselas volcanic sequence of the Hazelton Group is located within the Intermontane Stikine Terrane in the western part of the Usk map-area in north-western British Columbia. It is surrounded by intrusive units to the north and south and by Hazelton Group volcanic rocks of the Telkwa Formation to the east. Telkwa and Kitselas rocks are coeval in age; however, the primary relationship between the two map units is enigmatic due to a structural contact and differences in composition and metamorphic grade. The objective of this thesis was thus to characterize the Kitselas volcanic rocks in terms of volcanology, petrography, and geochemistry and to use this data to determine the primary relationship between Kitselas and Telkwa rocks. The field and petrographic characteristics are consistent with a model wherein the Kitselas volcanic rocks comprise the foot-wall of a detachment fault system, which includes the Usk Fault. The geochemical characteristics of the Telkwa and Kitselas volcanics indicate that rocks from both of these map units are part of a volcanic arc calc-alkaline suite and their trace element similarities indicate that they are genetically related.

December, 4, 2006

Keywords: Telkwa Formation, Kitselas Volcanic Sequence, Stikine Terrane, geochemistry, volcanology, petrography, and calc-alkaline.



## Table of Contents

|   |        |
|---|--------|
| Abstract  | 1.0    |
| Introduction  | 1.0    |
| Regional Geology  | 2.0    |
| The Canadian Cordillera                                 | 2.1    |
| Stikinia and the Hazelton Group                         | 2.2    |
| The Telkwa Formation                                    | 2.3    |
| Local Geology   | 3.0    |
| Previous Work: The Telkwa Formation in the Usk Map-Area | 3.1    |
| Stratified Units  | 3.2    |
| The Basal Conglomerate                                  | 3.2.1  |
| OK Range and Treasure Mountain                          | 3.2.2  |
| Kleanza Creek and Mount Pardek Section                  | 3.2.3  |
| Mt O'Brian Section                                      | 3.2.4  |
| Previous Work: The Kitselas Volcanic Sequence           | 3.3    |
| Field Observations: The Kitselas Volcanic Sequence      | 3.4    |
| Stratified Units  | 3.5    |
| Felsic Units  | 3.5.1  |
| Mafic Units   | 3.5.2  |
| The Usk Shear Zone                                      | 3.6    |
| Petrography   | 4.0    |
| Kitselas Andesites and Basalts                          | 4.1    |
| Mineralogy and Textures                                 | 4.1.1  |
| Plagioclase   | 4.1.11 |
| Quartz  | 4.1.12 |
| Pyroxene  | 4.1.13 |
| Secondary Minerals                                      | 4.1.14 |
| Kitselas Rhyodacites and Rhyolites                      | 4.2    |
| Mineralogy and Textures                                 | 4.2.1  |
| Quartz  | 4.2.11 |
| K-Feldspar  | 4.2.12 |
| Plagioclase   | 4.2.13 |
| Telkwa Andesites and Basalts                            | 4.3    |
| Mineralogy and Textures                                 | 4.3.1  |
| Plagioclase   | 4.3.1  |
| Clinopyroxene   | 4.3.12 |
| Quartz  | 4.3.13 |
| Composition of Lapilli                                  | 4.3.14 |

|   |        |
|---|--------|
| Secondary Minerals  | 4.3.15 |
| Telkwa Rhyolites  | 4.4    |
| Mineralogy and Textures   | 4.4.1  |
| Quartz  | 4.4.11 |
| K-Feldspar  | 4.4.12 |
| Plagioclase   | 4.4.13 |
| Clasts  | 4.4.14 |
| Secondary Minerals  | 4.4.15 |
| Intermediate Telkwa Sample  | 4.5    |
| Mount Pardek Sample   | 4.6    |
| Geochemistry  | 5.0    |
| Experimental Methods  | 5.1    |
| Post Magmatic Alteration  | 5.2    |
| Rock Type Classification  | 5.3    |
| Discussion  | 6.0    |
| Basalt Classification   | 6.1    |
| Determining the Tectonic Setting Using Discrimination Diagrams  | 6.2    |
| Normalized Trace Element Diagrams   | 6.3    |
| Interpreting Trace Element Patterns   | 6.3.1  |
| Trace Element Patterns of the Telkwa and Kitselas Volcanics   | 6.3.2  |
| Tectonic Implications   | 6.3.21 |
| Primary Relationship of Telkwa and Kitselas Samples   | 6.3.22 |
| Normalized Rare Earth Element Diagrams  | 6.4    |
| The Rare Earth Elements   | 6.4.1  |
| Interpreting Normalized Rare Earth Element Diagrams   | 6.4.2  |
| REE Patterns in the Telkwa and Kitselas Volcanic Rocks  | 6.4.3  |
| A Comparison of the Field and Petrographic Characteristics of Felsic Rocks from the Kitselas Volcanic Sequence and Telkwa Formation | 6.5    |
| A Comparison of the Field and Petrographic Characteristics of Mafic Rocks in the Kitselas Volcanic Sequence and Telkwa Formation    | 6.6    |
| Sources of Error  | 6.7    |
| Summary and Conclusion  | 7.0    |
| Acknowledgments   | 8.0    |
| References  | 9.0    |

## (1.0) Introduction

The Kitselas volcanic sequence of the Hazelton Group lies within the Intermontane Stikine Terrane in the western portion of the Usk map-area, north-western British Columbia (figure 1). Kitselas rocks are primarily rhyodacitic to rhyolitic flows, lapilli tuffs, and welded tuffs, but also include rare beds of crystal/ash tuffs and resedimented volcanics. Minor mafic flows are basaltic to andesitic in composition. The Kitselas volcanic sequence is surrounded by intrusive rocks to the north and south and by mafic to felsic volcanogenic rocks of the Telkwa Formation to the east (Nelson et al., 2005).

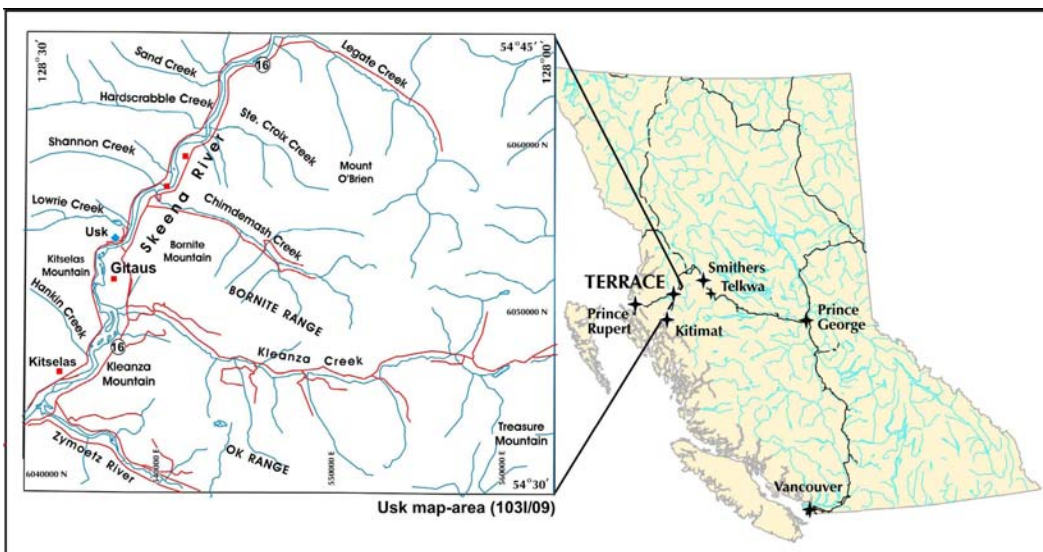


Figure 1: The Usk map-area is located close to Terrace, British Columbia (Nelson et al., 2005).

Kitselas and Telkwa rocks are roughly coeval in age. Gareau et al. (1997) reported U-Pb zircon dates of  $195 \pm 2.0$  Ma and  $193.9 \pm 2.1/-0.6$  Ma from two Kitselas rhyolites, whereas volcanic rocks of the Telkwa Formation are estimated to be Late Triassic to Earliest Jurassic in age (Gareau et al., 1997). The relationship between Kitselas and Telkwa rocks is, however, poorly understood due to differences in

composition, metamorphic grade, and deformational features (Gareau et al., 1997). Gareau et al. (1997) discovered that unlike other rocks of the surrounding Stikine Terrane, which are mainly undeformed and zeolite to prehnite-pumpellyite metamorphic grade, volcanic rocks of the Kitselas sequence had been ductily deformed and locally metamorphosed to greenschist facies. Kitselas rocks are in fault contact with rocks of the Telkwa formation and the orientation of deformational fabrics have led to the suggestion that the Kitselas volcanic rocks lie within a block that has been tectonically exhumed into its current position; the Kitselas volcanic rocks comprise the foot-wall of a detachment fault system (Gareau et al., 1997). The objective of this thesis is to characterize the Kitselas volcanic rocks in terms of volcanology, petrography, and geochemistry and to use this data to determine the primary relationship between the Kitselas volcanic sequence and rocks of the Telkwa Formation. Characterization of the Kitselas volcanic sequence and the determining of its relationship to rocks of the Telkwa Formation may lead to a better understanding of the nature and paleogeography of Telkwa volcanism.

## **(2.0) Regional Geology**

### **(2.1) The Canadian Cordillera**

The Mid Proterozoic to Cenozoic Canadian Cordillera comprises western most Canada (Gabrielse and Yorath, 1992). This region has been divided into five north-south trending morphogeologic belts that are referred to as, from east to west, the Foreland Belt, the Omineca Belt, the Intermontane Belt, the Coast Belt, and the Insular Belt (figure 2) (Gabrielse and Yorath, 1992). The Foreland Belt represents an ancient passive continental margin that was detached, folded, and thrust onto the North American

craton. The Omineca Belt is primarily composed of metamorphic and granitic rocks and contains the boundary between continental rocks of both new and ancestral North America (Gabrielse and Yorath, 1992). The Intermontane Belt is composed of Devonian to recent volcanic and sedimentary rocks and Early Mesozoic to Early Tertiary plutonic rocks; its components have been derived from the accretion of many outboard terranes to ancestral North America (Gabrielse and Yorath, 1992). Rocks of this belt rarely reach greenschist metamorphic grade (Gabrielse and Yorath, 1992). The Intermontane Belt represents a topographic low in comparison to its neighbouring Omineca and Coast Belts. Boundaries in the southeast are represented by changes in lithology and topography whereas the north-eastern boundaries are defined by a series of regional strike-slip faults. The south-western extent of the Intermontane Belt is also fault bounded whereas the more north-western limits are represented by a transition from low lying volcanic and sedimentary rocks to high relief granites belonging to the Coast Belt (Gabrielse and Yorath, 1992). The Coast Belt is a large continental-margin batholith that extends from Yukon Province to north-western Washington State; rocks of this belt are the result of the subduction and/or accretion of the Insular Belt to the Intermontane Belt (Gabrielse and Yorath, 1992). The Coast Belt is mainly composed of Cretaceous and Tertiary granitic and metamorphic rocks. Metamorphism reached upper amphibolite facies suggesting that Coast Belt rocks have been subjected to greater burial depths and uplift with respect to rocks of adjacent belts. The south-western boundary lies just off the coast of

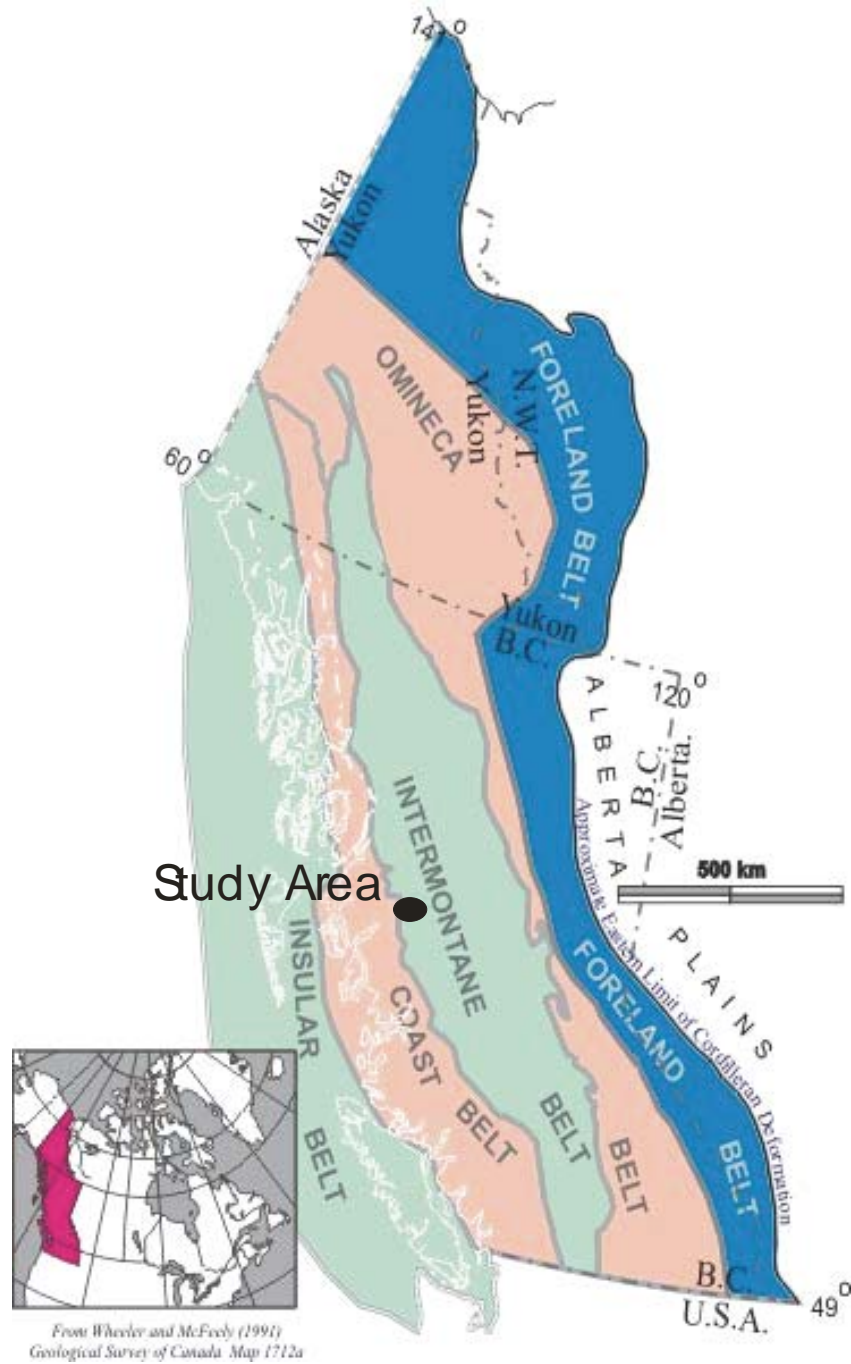


Figure 2: The five belts of the Canadian Cordillera are, from east to west, the Foreland Belt, the Omineca Belt, the Intermontane Belt, the Coast Belt, and the Insular Belt. The study area is located within the Intermontane Belt proximal to the Skeena River (Diagram from GSC, 2006).

mainland British Columbia and the more northern boundaries are defined by faults (Gabrielse and Yorath, 1992). Rocks of the Insular belt are exposed in the mountains of Vancouver Island, the Queen Charlotte Islands, and the Alexander Archipelago in the Alaska Panhandle. These rocks are volcanic, sedimentary, and plutonic and are Paleozoic, Mesozoic, and Cenozoic in age. The western boundaries of this belt are located at the base of the continental slope (Gabrielse and Yorath, 1992).

## **(2.2) Stikinia and the Hazelton Group**

Rocks of the Canadian Cordillera have developed in different depositional or volcanic settings and paleogeographical locations. The belts have therefore been divided into different terranes to better characterize the rocks within them. Moores and Eldridge (1995) have defined a terrane as a collection of rocks bounded by sutures and containing a stratigraphy, petrology, and/or paleolatitude distinct from those of neighbouring terranes.

The Stikine Terrane (Stikinia) is the largest (2000 × 300 km) accreted terrane in British Columbia and is a major component of the Intermontane Belt (figure 3) (Mardson and Thorkelson, 1992). This terrane is composed of Lower Devonian to Middle Jurassic volcanic, sedimentary, and plutonic rocks of island arc origin (Gabrielse and Yorath, 1992). Stikinia's main constituents include the Devonian to Permian Stikine Assemblage, the upper Triassic Stuhini Group, and the Lower to Middle Jurassic Hazelton Group (Anderson, 1989). The eastern boundary of the Stikine Terrane is a fault contact with the Cashe Creek Terrane. The details of the western boundary are blurred due to Cretaceous and Tertiary plutonism and metamorphism in the Coast Belt.

The Hazelton Group is characterized by basaltic to rhyolitic volcanic flows, pyroclastic rocks, and sedimentary strata that were deposited in the Hazelton Trough between the Lower and Middle Jurassic (Tipper and Richards, 1976). Rocks of the

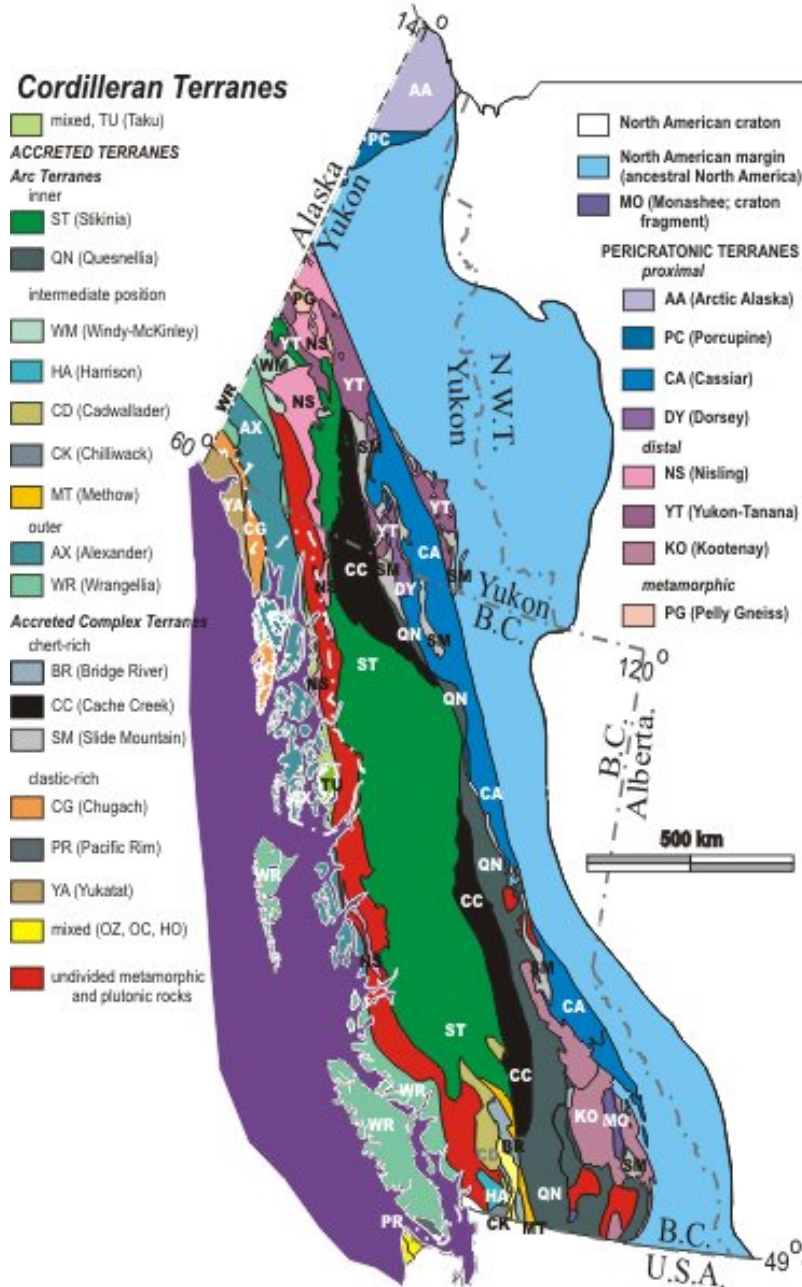


Figure 3: The Stikine Terrane is British Columbia's largest accreted terrane and is composed of volcanic, plutonic, and sedimentary rocks of island arc origin (Diagram from GSC, 2006).



### **(2.3) The Telkwa Formation:**

The Telkwa Formation is the most immense and extensive Formation of the Hazelton Group, as it has been deposited across the entire width of the Hazelton Trough (Richards and Tipper, 1976). The Telkwa Formation forms the base of the Hazelton Group and is overlain by the Nilkitkwa Formation (Richards and Tipper, 1976). It is characteristically composed of red, maroon, purple, grey, and green, calc-alkaline basalt to rhyolite flows and pyroclastic rocks with lesser intravolcanic sedimentary rocks (Gabielse and Yorath, 1992). The thickness of the Telkwa Formation is variable but reaches up to 400m southwest of the Smithers area (Gabielse and Yorath, 1992).

### **(3.0) Local Geology**

#### **(3.1) Previous Work: The Telkwa Formation in the Usk Map Area**

Nelson et al. (2005) completed previous work on the Telkwa Formation in the Terrace area in the summer of 2005. Mapping at a 1:50 000 scale was conducted on a 560 km<sup>2</sup> area in an attempt to better understand the character and paleogeography of Telkwa volcanism (Nelson et al., 2005). The results of this study are described below and the finished map product is shown in figure 5. The reader is referred to Nelson et al. (2005) and Baressi and Nelson (2005) for further information.

#### **(3.2) Stratified Units**

##### **(3.2.1) The Basal Conglomerate**

The basal contact of the Telkwa Formation is exposed at the base of the western O. K. Range. It consists of a Jurassic polymictic conglomerate that unconformably overlies thrust-imbricated Triassic and Paleozoic strata (Nelson et al., 2005). Clast

composition is variable; in general, intraformational clasts consist of andesite, dacite and rhyolite whereas extraformational clasts, derived from underlying Permian volcanoclastic rocks, consist of limestone, black chert, andesite, dacite, and rhyolite (Nelson et al., 2005). Faint differences in composition and texture distinguish intraformational clasts from extraformational clasts. For example, lath-shaped plagioclase phenocrysts are predominant in the basal Telkwa Formation, whereas clinopyroxene and quartz phenocrysts are typical of the underlying Permian rocks (Nelson et al, 2005).

### **(3.2.2) OK Range and Treasure Mountain**

This section is composed of easterly dipping maroon and green andesitic volcanoclastic rocks, lesser andesite flows, rare thin beds of volcanic derived sedimentary rocks, and dacitic lapilli and crystal ash tuffs (Nelson et al., 2005). Pyroclastic and epiclastic deposits were distinguished from one another using Jocelyn McPhie's (1993) set of criteria. For example, pyroclastic deposits lack textures typical of resedimented rocks such as grading, laminar bedding, and sorting. There is no evidence of significant transport or reworking of clasts prior to deposition in pyroclastic rocks. Some tuffs, both in this section and in the rest of the map-area, are welded and only non-welded clasts can be resedimented (McPhie, 1993). Rocks in the OK Range and Treasure Mountain section reach a minimum thickness of about 4.7 km in the southeast corner of the map sheet where Treasure Mountain is located.

Andesitic lapilli tuffs are monomictic to polymictic. Lapilli are characteristically plagioclase-phyric. Phenocrysts are typically euhedral, lath-shaped,

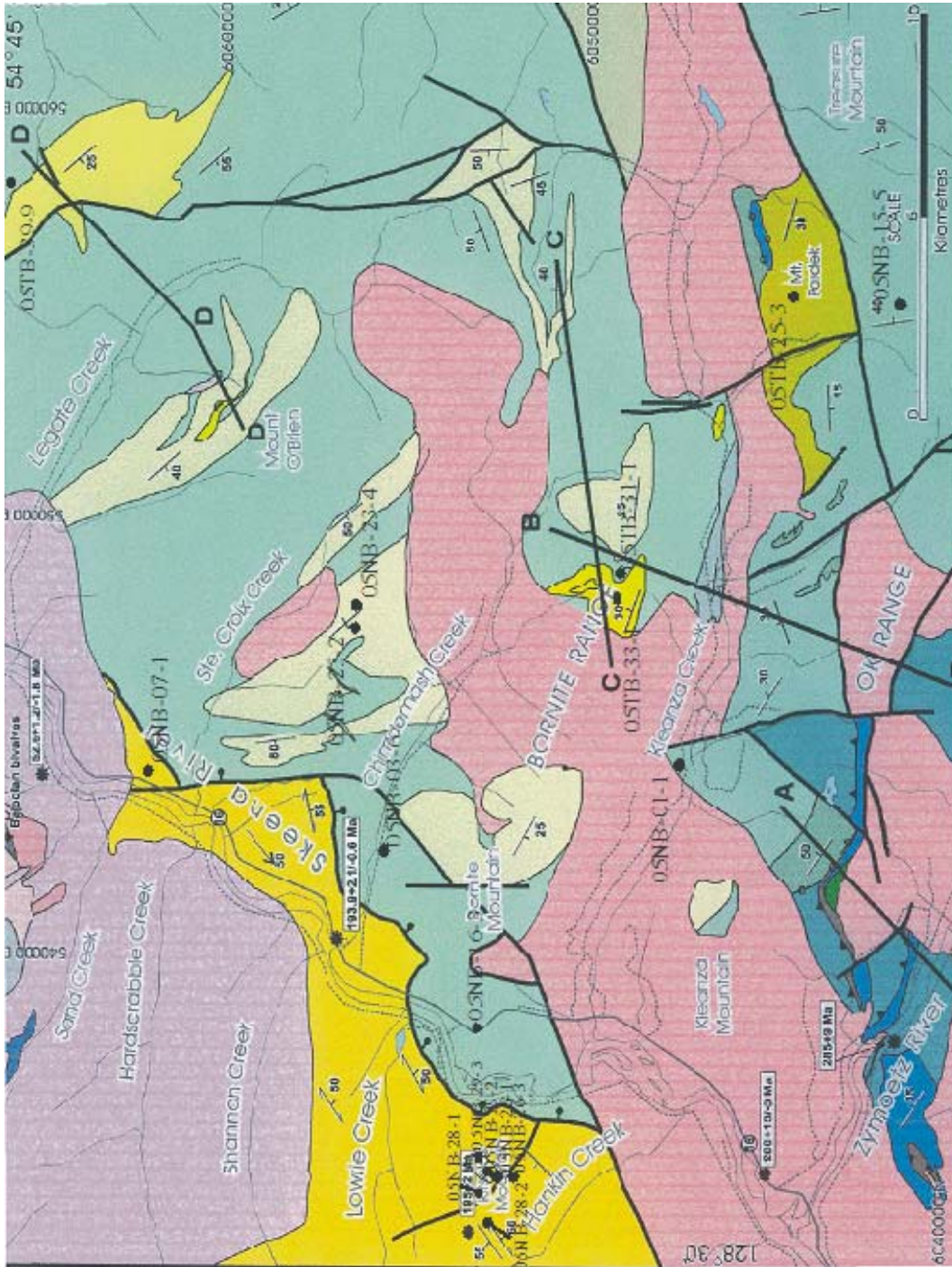
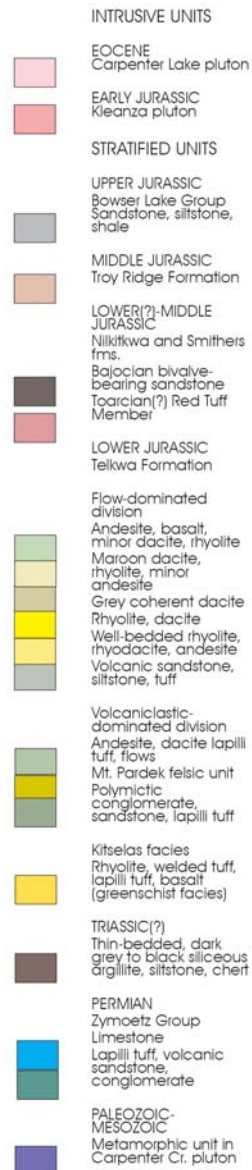


Figure 5: Final map product of the Usk map-area. The Kitselas volcanic sequence is highlighted in yellow and surrounded by plutonic rocks to the north and south and by volcanic rocks of the Telkwa Formation to the east. The corresponding legend is located on the following page (Nelson et al., 2005).



and vary between lengths of 2 and 5 mm. Rare redundant hornblende and clinopyroxene phenocrysts were also identified (Nelson et al., 2005).

Flows are massive, planar to lensoid, locally amygdaloidal, and 20 to 200 m thick. These flows are locally brecciated and grade into lapilli tuffs with which they share the same textural characteristics (Nelson et al., 2005).

Thin beds of volcanic sandstone, siltstone, and mudstone are interpreted to have been deposited during quiescent intervals within a subaqueous setting, as these beds contain rip-up clasts and show graded bedding (Nelson et al., 2005).

Dacitic volcanic rocks are maroon, brick red, light grey, lavender, and pink; most are lapilli and crystal ash tuffs although rare massive flows are also present. Lapilli tuffs are monomictic to polymictic and are in some cases welded. Clasts are siliceous, aphanitic to glassy, and sometimes contain very small (< 1 mm) feldspar phenocrysts. Massive dacites have similar compositions (Nelson et al., 2005).

### **(3.2.3) Kleanza Creek and Mt Pardek Section**

This section occupies the southern slopes of the Kleanza Creek valley and extends from Kleanza Mountain to Mt Pardek (Nelson et al., 2005). The western part of this section is mainly composed of andesitic lapilli tuffs with lesser interbedded volcanic sandstone and siltstone. A felsic tuff base overlain by intermediate volcanoclastic rocks and volcanic-derived sedimentary strata characterizes the eastern segment (Nelson et al., 2005).

The felsic tuff sequence of Mt. Pardek was deposited in a subaqueous environment and is composed of quartz-feldspar-phyric flows, tuffs, and resedimented volcanic rocks. These tuffs are typically pastel green in colour and uniquely contain up to 60% clear, euhedral quartz crystals. Mt. Pardek rocks are sometimes colour banded, have a waxy translucent appearance, and are monomictic to polymictic with rhyolite and quartz clasts (Nelson et al., 2005).

### **(3.2.4) Mt O'Brian Section**

The Mt O'Brian section is an extensive zone that spans from just north of

Kleanza Creek to the northern and eastern borders of the Usk map area. Although lapilli tuffs are common, this subdivision is dominated by andesite and dacite volcanic flows rather than volcanoclastic rocks and is thus thought to represent proximity to volcanic centres (Nelson et al., 2005).

Textural changes in this section are partly represented by sub-hedral to euhedral and tabular rather than lath shaped plagioclase phenocrysts. The size of plagioclases varies from a few mm to over a cm in length (Nelson et al., 2005). Andesite flows are predominantly amygdaloidal; amygdules are typically irregular in shape, less than a mm to many cm in diameter, and filled with zeolite +/- quartz +/- epidote +/- chlorite +/- pumpellyite (Nelson et al., 2005).

Massive dacite flows, flow breccias, lapilli tuffs and welded tuffs with lithic and pumice fragments, and minor crystal tuffs are aphyric to finely porphyritic. These dacites have very similar textures to those in the Kleanza Creek section. They are maroon, brick red, and pastel lavender, pink, orange and cream in colour (Nelson et al., 2005).

Rhyolite centres are located in the middle of the Bornite Range, north of Mt O'Brian between Ste. Croix and Legate Creeks, and in the northeast corner of the Usk Map area (Nelson et al., 2005). Lapilli tuffs are unwelded to strongly welded with lithic and pumice fragments. Massive rhyolites form thin flows, flow breccias, minor domes, and cryptodomes. Rhyolite lapilli tuffs and massive rhyolites are highly siliceous, aphanitic, often flow banded, semi-translucent, and white, pink, orange, lavender, or brick red in colour (Nelson et al., 2005). Resedimented felsic volcanic rocks range from conglomerates to sandstones. Lastly, aphanitic and highly siliceous rhyolites may be felsic ash tuffs or exhalative cherts (Nelson et al., 2005).

### **(3.3) Previous Work: Rocks of the Kitselas Volcanic Sequence**

Previous 1:1000 scale surface geological mapping on Kitselas Mountain was conducted by Carter (1970). The lower unit of Kitselas Mountain was described as being composed of rhyolite-dacite crystal-lithic tuff and breccia. Fragment size differentiated two main varieties of these volcanic rocks; one type contained fragments of one cm or more in length and the other was composed of tuff sized fragments ( $> 2$  mm) (Leyrit and Montecat, 2000) (Carter, 1970). Massive basalts and basaltic andesites were found to unconformably overlie the felsic sequence. These rocks were described as apple green to dark grey flow breccias and purple tuff breccias (Carter, 1970). Other lithologies reported include an andesitic feldspar porphyry sill located on the south-eastern slope of Kitselas Mountain and minor diorite dykes found adjacent to a northwest striking fault on the southwest side of the Kitselas Mountain peak (Carter, 1970). Carter (1970) also described two mineralized zones, which are referred to as the A and B zones; these are respectively located to the east and south of the Kitselas summit. Trenching and diamond drilling have been used to explore both zones. Mineralization in the A zone is characterized by the concentration of chalcopyrite, bornite, and possibly tetrahedrite within fractures and shear planes of felsic volcanic rocks. Copper-silver mineralization is found along the margins of and adjacent to diorite dykes in the B zone (Carter, 1970). Copper mineralization has also been observed in rhyolites to the west of the Kitselas peak and in association with mafic dykes (Carter, 1970).

### **(3.4) Field Observations: The Kitselas Volcanic Sequence**

The Kitselas volcanic sequence is a thick predominantly felsic ( $>95\%$ ) sequence that is exposed on Kitselas Mountain, on the Ridge between Shannon and Lowrie Creek,

and east of the Skeena River between Usk and the ridge north of Ste. Croix Creek. This sequence reaches a minimum thickness of approximately 3 km from the west side of the Skeena River to the western edge of the map sheet. The Kitselas volcanic deposits are composed mostly of rhyodacites and rhyolites, accompanied by rare dacites; however, they also include minor basalts and andesites (figure 6). Pyroclastic beds predominantly dip homoclinally between 50° and 70° to the northwest and strike between 220° and 245° (figure 7). The lowest exposed part of this sequence, which outcrops east of the Skeena River and at the bottom of Kitselas Mountain, is entirely comprised of massive rhyodacites, whereas rocks further up in the section are principally thick-bedded felsic volcanoclastics and minor flows.

### **(3.5) Stratified Units**

#### **(3.5.1) Felsic Units**

Massive rhyodacites are characteristically translucent to opaque, medium grey to light purple in colour, and aphanitic. They contain up to 10% tabular to equant feldspar microphenocrysts of up to 2 mm in length. Rhyolite flows further up-section have a similar composition to massive bodies but are flow and colour banded on a mm to cm scale with average band widths between 2 and 10 mm.

Rhyolitic volcanoclastic rocks are lapilli tuffs, welded tuffs, and minor beds of crystal and /or ash tuffs and resedimented volcanics. Tuffs are predominantly monolithic<sup>1</sup>. Lapilli are siliceous, glassy to aphanitic, and white, light to medium purple, or grey to blue-grey in colour. Lapilli locally contain rare feldspar phenocrysts with similar characteristics to those found in massive bodies and are typically composed of

---

<sup>1</sup> The term monolithic was used in the field to describe clasts, lithics, and phenocrysts that differ slightly in appearance, shape, and/or texture, but that are actually of the same chemical and/or mineralogical composition.

rhyodacite/rhyolite or pumice. Rare scoriaceous bombs exhibiting concavo-convex boundaries are present in one clast-rich rhyodacitic to dacitic lapilli tuff outcrop. The overall abundance of lapilli varies between about 5 and 50% but typically accounts for about 20% of the volume of felsic volcanoclastic rocks on Kitselas Mountain. Lapilli are angular to rounded and sand to pebble size, but are predominantly between 0.5 and 3 cm in diameter. Welded tuffs show eutaxitic textures with typical aspect ratios of fiamme between approximately 1:8 and 1:20 (figure 8). Groundmasses may be light grey, light grey-blue, light grey-purple, and white in colour. Lapilli and their host rock tend to share very similar textures and colours and appear to be of the same composition.

One outcrop, which is located on the western ridge of Kitselas mountain, is about 100 m thick, very well bedded (on a mm to 10's of cm scale) and colour banded. Alternating zones of homogeneous siliceous and pyroclastic material exhibit both normal and normal-reverse grading. These features are suggestive of ash flows or ignimbrite origin. When debris moves as a strong mass flow, rather than just being deposited in a simple or regular manner, traction causes larger materials to be sorted into a higher level where shear flow is weaker (Branney and Kokelaar, 2002; Bagnold, 1954). Homogeneous glassy beds may represent intensely welded sections. This outcrop tends to more colourful than other highly siliceous volcanoclastic rocks on Kitselas Mountain; its components are also mint green and light pink in addition to white, grey, and purple (figures 9 and 10).

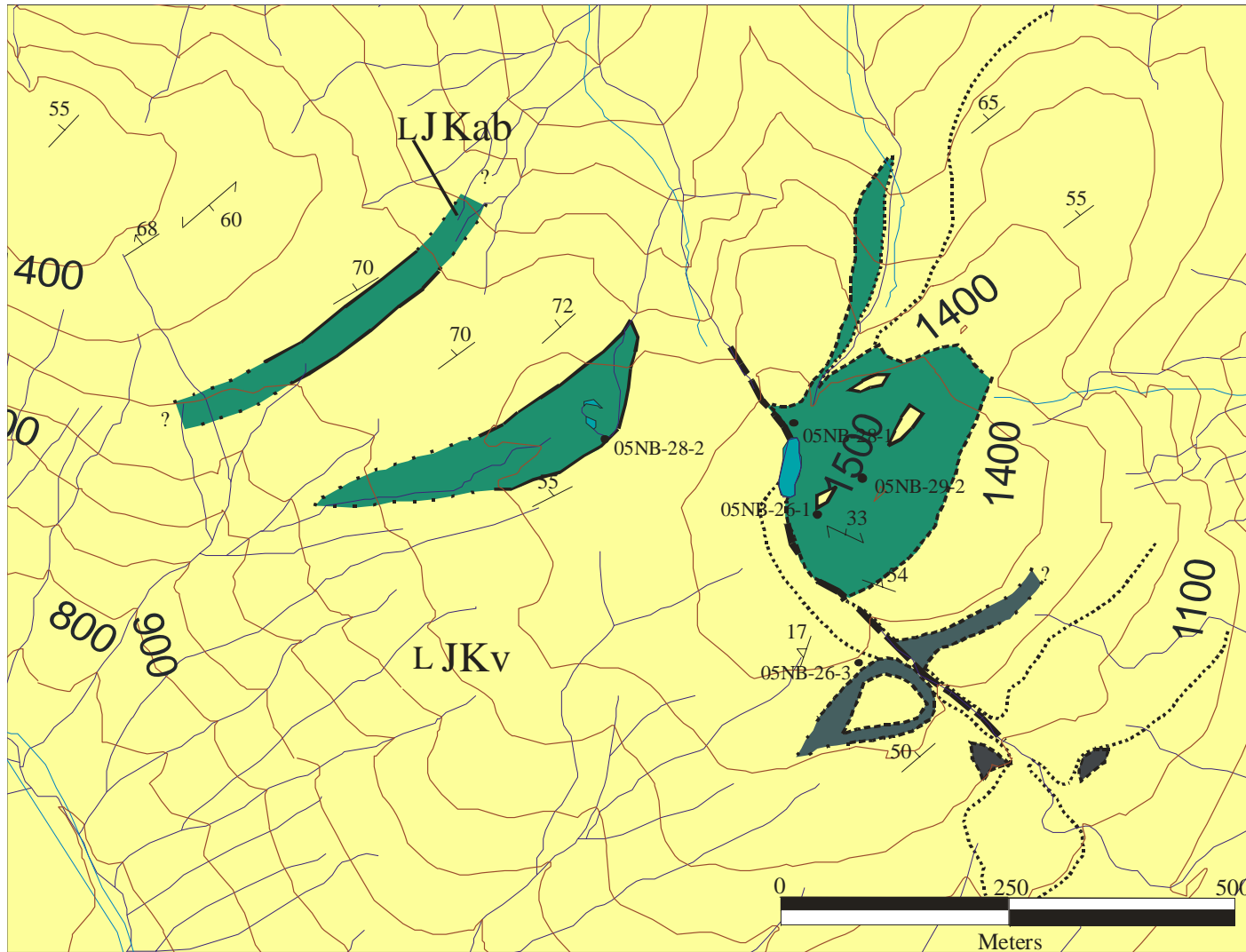


Figure 6: The Kitselas unit, which is highlighted in yellow, is primarily composed of felsic volcanoclastic rocks. The minor mafic component shown in the lighter shade of green outcrops on the summit of Kitselas Mountain and the mountain's western ridge, whereas diabase dykes outcrop on the south-eastern slope. The corresponding legend is located on the following page.

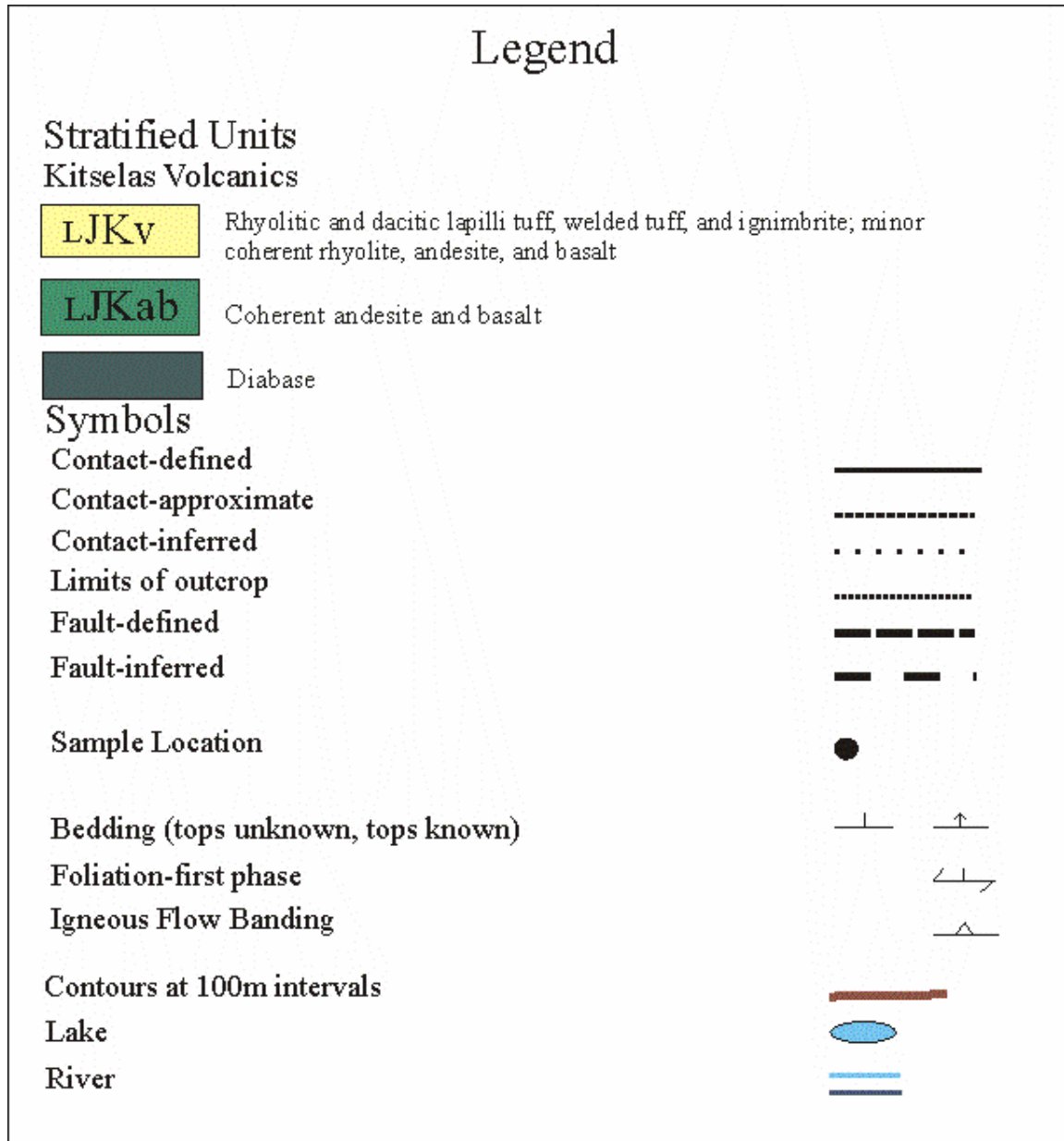




Figure 7: Homoclinal bedding of volcaniclastic rhyolites is well exposed on the flanks of the north-western ridge of Kitselas Mountain; beds all dip steeply to the north-northwest. Photo courtesy of J. Nelson, 2005.

Up-section in the Kitselas sequence lays one thin bed of resedimented volcanics which grades upwards from a laminated mudstone base to a clast supported conglomerate. This conglomerate layer is approximately a couple of meters in thickness and its matrix is composed of white to light blue-grey sandstones, siltstones, and mudstones. Volcanic clasts are siliceous, glassy, aphanitic, homogeneous, and/or colour and flow banded and are typically various shades of white, grey, blue, and less commonly beige. They are sub-angular to sub-rounded and average about 2-3 cm in diameter at the bottom to 2-3 mm at the top of the unit (figure 11). Finer underlying beds are of a similar



Figure 8: Welding of rhyodacitic tuffs is especially common on the eastern to south-eastern flanks of Kitselas Mountain. Fiamme, which are darker grey-blue in color, have typical aspect ratios between approximately 1:8 and 1:20. The portion of the pen shown in this photograph is approximately 9 cm in length. Photograph courtesy of J. Nelson, 2005.



Figures 9 and 10: A layered ash flow tuff outcrops on the western ridge of Kitselas Mountain. Photographs courtesy of J. Nelson, 2005

composition; sand beds are up to about 40 cm thick whereas silt and mud beds vary in thickness from 1 mm to just under a cm. Flame structures, load casts, and cross beds observed in this section are suggestive of a subaqueous depositional environment involving water currents.

Several small dacitic lapilli tuffs outcrop on the north-northwest ridge of Kitselas Mountain. They are poly lithic rather than monolithic and sometimes contain grainy/possibly hypabyssal lapilli in addition to massive felsic lapilli and pumice clasts. The colour of these tuffs is also more variable, ranging from maroon to purple and beige to white and grey.

### **(3.5.2) Mafic Units**

Three continuous but thin (60 to 250m) units of the Kitselas volcanic sequence are more mafic in composition. The thickest of these units caps the summit of Kitselas Mountain and is andesitic in composition. Textures and colours in this unit vary from one outcrop to the next. For example, andesites adjacent to the south-eastern side of Kitselas Lake are aphanitic, medium grey blue in colour on fresh surfaces, and plagioclase-phyric containing up to 10% euhedral to subhedral plagioclase phenocrysts of about 2 to 3 mm in length. Andesites further to the southeast and to the west are locally vesicular and amygdaloidal, have a deep dark grey blue colour, and tend to lack the plagioclase phenocrysts found in outcrops closer to Kitselas Lake; when phenocrysts are present, they are thoroughly epidotized microphenocrysts. Just north of the Kitselas summit, andesites are characteristically aphanitic and medium grey in colour with local patches of pistachio green, which likely represent epidotization. Plagioclase microphenocrysts in these outcrops are often thoroughly epidotized. To the east of the Kitselas summit, one

andesitic outcrop has smaller and a lesser proportion of amygdules and vesicles and is holocrystalline as opposed to aphanitic. It is also thoroughly epidotized and has been left with a brilliant pistachio green colour. No definite contacts could be drawn between these rocks and mafic rocks in adjacent outcrops. It is thus proposed that they represent proximity to eruptive fissures or centres where hydrothermal fluids (and thus hydrothermal alteration) would be concentrated (Winter, 2001).

The other two mafic units outcrop on the western ridge and are basaltic in composition. These volcanic rocks are dark shades of deep blue-grey to dark grey-green. They lack plagioclase phenocrysts and are characterized by aphanitic, hackly, and vesicular to scoriaceous textures (figure 12). Minor diabase dikes are found on the south-eastern slope of Kitselas Mountain and thin concordant mafic flows or sills outcrop on the eastern slopes of the Skeena River.

### **(3.6) The Usk Shear zone**

The Usk fault, which separates Kitselas volcanic rocks from Telkwa rocks of the Mount O'Brian section, generally dips shallowly to the southeast and is offset by the Gitaus and Tumbling Creek faults (Nelson et al., 2005). Bedding attitudes rapidly change from one side of the fault to the other, as Kitselas beds strike towards the south-west and dip to the north-west while those of the Telkwa Formation strike to the south-east and dip to the south-west. The Usk fault also juxtaposes rocks of different metamorphic grades (Nelson et al., 2005). The change from zeolite facies in the Telkwa Formation to greenschist facies in the Kitselas volcanic sequence appears to be transitional, as metamorphic actinolite is found in some Telkwa andesites/basalts up to about 300m from the fault (Nelson et al., 2005). Kitselas rocks locally contain south-easterly dipping and



Figure 11: Base of the clast supported volcanic conglomerate that outcrops on the western ridge of Kitselas Mountain. The scale used was a pen of approximately 13.5 cm in length. Photograph courtesy of J. Nelson, 2005.



Figure 12: Base of a thin scoriaceous basalt layer located on the western ridge of Kitselas Mountain. The scale used was a pen of approximately 13.5 cm in length. Photograph courtesy of J. Nelson, 2005.

strong penetrative cleavage; foliations are most pronounced in highway outcrops north of Chimdemash Creek and on the northern to eastern flanks of Kitselas Mountain (Nelson et al., 2005). The shear zone of the Usk fault is hundreds of meters wide and is represented by strong cleavage and brittle shears in rocks of the Telkwa Formation (Nelson et al., 2005).

#### **(4.0) Petrography**

Petrographic analysis was conducted on 17 thin sections; 8 of these represent rocks of the Kitselas volcanic sequence and the remaining represent the Telkwa Formation. All except two thin sections (05NB-16-3 and 05NB-29-3) come from samples that were analysed for geochemistry. These sections were used to determine the petrographical characteristics of mafic and felsic volcanic rocks from the Usk map area. The reader is referred to figure 5 and table 1 for sample locations and classification.

##### **(4.1) Kitselas Andesites and Basalts**

The mineralogical compositions of these rocks suggest that one is basaltic (05NB-28-2) and the other four are andesites (05NB-26-1, 05NB-29-2, 05NB-29-3, and 05NB-28-1). These samples are predominantly plagioclase porphyries with phenocryst content varying between 2 and 10 % (figure 13). Matrices are composed of plagioclase, clinopyroxene, and +/- minor quartz. Only one of the four thin sections is vesicular. These mafic rocks have metamorphic mineral assemblages typical of greenschist facies, including varying proportions of actinolite, epidote, and chlorite.

Table 1: A list of samples used in this project, their geographical origins, and their rock type based on field observations, petrography, and geochemistry (see sections ahead).

| Sample #  | Telkwa or Kitselas | Sample Location                           | Rock Classification           |
|-----------|--------------------|---|-------------------------------|
| 05NB-01-1 | Telkwa             | Kleanza Creek                             | Andesite Flow                 |
| 05NB-03-6 | Telkwa             | Chimdemash Cr.                            | Basalt Flow                   |
| 05NB-07-1 | Kitselas           | Ste. Croix Cr.                            | Rhyodacite/Rhyolite – Massive |
| 05NB-15-5 | Telkwa             | Treasure Mountain                         | Andesite Flow                 |
| 05NB-16-3 | Telkwa             | Hwy-between Kleanza and Chimdemash Creeks | Andesite Lapilli Tuff         |
| 05NB-23-2 | Telkwa             | Ste. Croix Cr.                            | Rhyolite - Massive            |
| 05NB-23-4 | Telkwa             | Ste. Croix Cr.                            | Dacite Flow                   |
| 05NB-26-1 | Kitselas           | Kitselas Mountain                         | Andesite Flow                 |
| 05NB-26-3 | Kitselas           | Kitselas Mountain                         | Rhyolite Flow                 |
| 05NB-28-1 | Kitselas           | Kitselas Mountain                         | Andesite Flow                 |
| 05NB-28-2 | Kitselas           | Kitselas Mountain                         | Basalt Flow                   |
| 05NB-29-2 | Kitselas           | Kitselas Mountain                         | Andesite Flow                 |
| 05NB-29-3 | Kitselas           | Kitselas Mountain                         | Andesite Flow                 |
| 05TB-25-3 | Telkwa             | Mount Pardek                              | Andesite - Pyroclastic        |
| 05TB-31-1 | Telkwa             | Bornite Range                             | Basalt Flow                   |
| 05TB-33-1 | Telkwa             | Bornite Range                             | Rhyolite Flow                 |
| 05TB-39-9 | Telkwa             | NE Mount O’Brian                          | Rhyolite - Massive            |

### **(4.1.1) Mineralogy and Textures**

#### **(4.1.11) Plagioclase**

The quantity of plagioclase varies from 35 to 68%. Crystals range in size from 0.03 to 0.09 mm in groundmasses whereas phenocrysts are between 0.19 and 0.59 mm. They are anhedral to euhedral although their boundaries are often irregular due to sericitization and rare saussuritization. Where crystal form is defined, plagioclases are lath shaped, elongate, and less commonly bladed. Crystals are often aligned resulting in a weak to strong trachytic texture. Plagioclase crystals are often poikilitic containing few to abundant inclusions of epidote and/or actinolite (figure 14). The original composition of these inclusions was likely pyroxene. Plagioclases typically display albite twinning.

#### **(4.1.12) Quartz**

Quartz is present in the groundmass of all but one of the samples. It is a minor component comprising only up to a maximum of 8% of the groundmass volume. Crystals range in size from 0.02 to 0.04 mm, are anhedral, and have irregular to serrated boundaries.

#### **(4.1.13) Pyroxene**

Samples have varying proportions of clinopyroxene. Clinopyroxene crystals comprise 2-40% of the groundmasses; pyroxene phenocrysts are scarce in these rocks. Crystals range in size between 0.05 and 0.09 mm. All pyroxenes have been at least partially, but most often completely, replaced by epidote and/or actinolite; therefore, primary textures are generally masked by alteration. In cases where epidote and/or actinolite pseudomorphs preserve crystal shape, they are euhedral and elongate with well-defined boundaries (figure 15).

#### **(4.1.14) Secondary Minerals**

Sericite replaces plagioclase in all of the Kitselas samples and constitutes between 2 and 20 % of the rock volumes. Sericite has a platy habit and often follows the alignment of plagioclase grains. Secondary ferromagnesian minerals include chlorite, epidote, and actinolite, an assemblage that is indicative of greenschist metamorphism (figure 16). Chlorite was identified in the samples that were collected from the Kitselas summit (samples 05NB-29-2 AND 05NB-29-3) and to the north-northeast of Kitselas Lake (05NB-28-1); this mineral comprises up to 10% of the rock volumes. Crystals are fibrous to anhedral with very irregular grain boundaries and are predominantly found disseminated throughout the groundmass. Epidote is present in all of the mafic Kitselas samples at variable concentrations and most commonly occurs as anhedral aggregates dispersed throughout the sample. The majority of epidote is likely replacing pyroxene as these two minerals are chemically compatible, however, epidote also locally pseudomorphs plagioclase. Actinolite occupies up to 22 % volume of the mafic rocks on Kitselas Mountain. It is moderately pleochroic and pale to medium green in plane polarized light. Crystals are typically acicular to bladed, but are also anhedral. This mineral is also thought to be replacing pyroxene. Ferromagnesian minerals are also found in vesicles along with secondary quartz. In this case, chlorite, epidote, and actinolite tend to be slightly coarser grained whereas quartz crystals are anhedral and tend to have serrated grain boundaries. Rare thin veinlets of quartz are approximately 0.05 mm wide. Rare anhedral carbonate crystals were identified in samples 05NB-26-1 and 05NB-28-1.

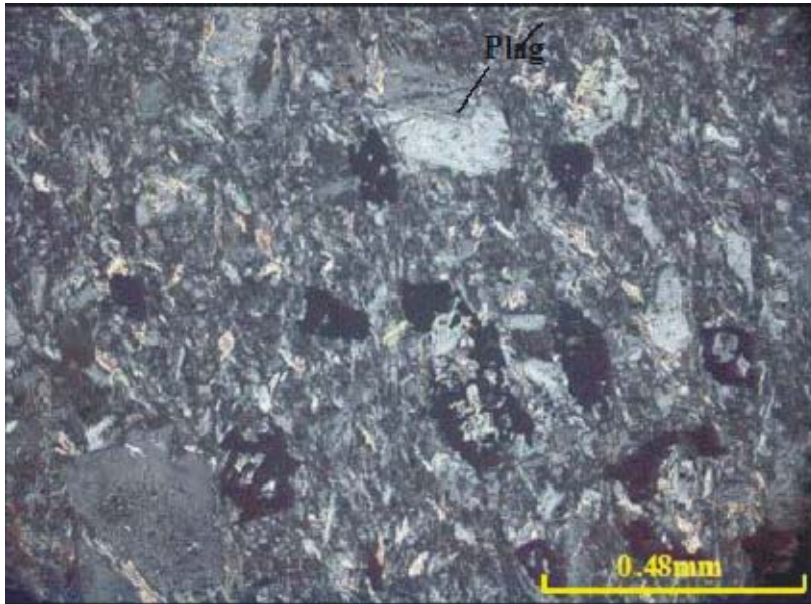


Figure 13: Typical petrographical characteristics of mafic rocks on Kitselas Mountain; this is a photograph of sample 05NB-28-2 taken at 10x magnification with crossed nicols.

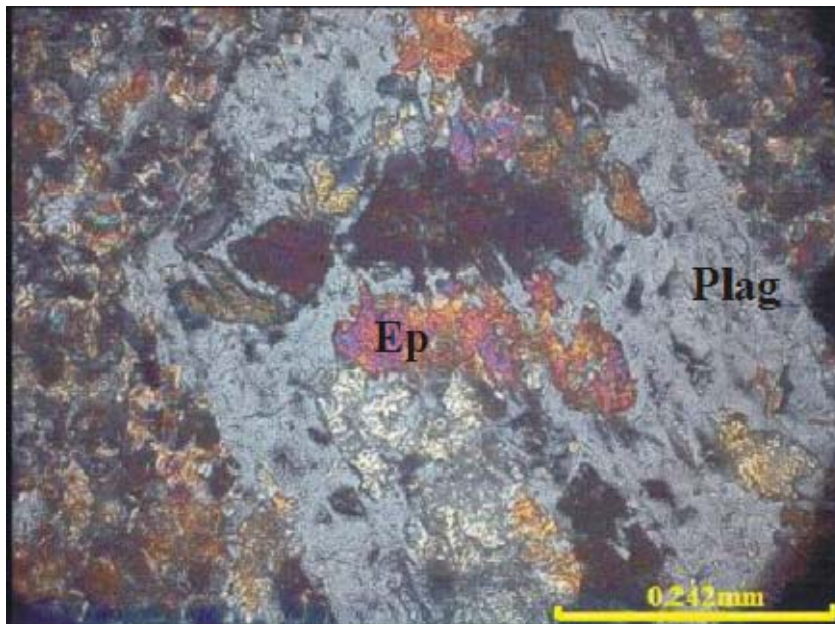


Figure 14: Plagioclase phenocrysts often contain few to abundant inclusions of epidote, the original composition of which was likely pyroxene. This photograph shows these inclusions in sample 05NB-26-3 at 20x magnification with crossed nicols.

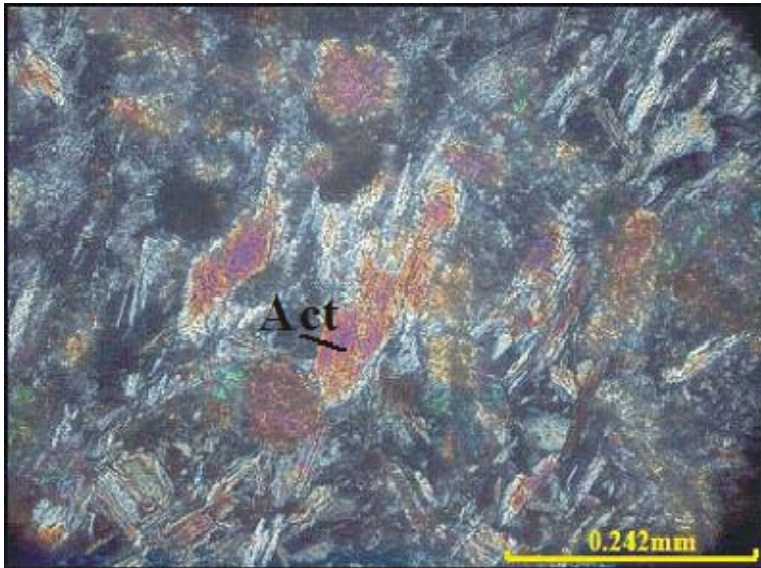


Figure 15: Actinolite replacing pyroxene in sample 05NB-29-3. This photograph was taken at 20x magnification with crossed nicols.



Figure 16: Mafic samples taken to the north, east, and south of Kitselas peak have metamorphic assemblages typical of greenschist facies; this sample (05NB-29-3) contains very high proportions of actinolite, epidote and chlorite. The photograph was taken at 10x magnification with crossed nicols.

## **(4.2) Kitselas Rhyodacites and Rhyolites**

One of the felsic Kitselas samples is rhyodacitic to rhyolitic and the other is a rhyolite. Felsic Kitselas samples are predominantly composed of potassium feldspar, quartz, and minor (up to 5%) plagioclase. Rare plagioclase phenocrysts are present in both lithologies, whereas phenocrysts of quartz and K-feldspar were only identified in massive rhyolites (sample 05NB-07-1) (figure 17). Groundmasses are either equigranular or seriate; the latter texture pertains to flow banded rhyolites (sample 05NB-26-3) in which discontinuous and thin bands of quartz crystals are progressively coarser grained than the thicker K-feldspar dominated bands (figure 18). Alteration of these samples is characterized by weak sericitization of both K-feldspar and plagioclase.

### **(4.2.1) Mineralogy and Textures**

#### **(4.2.11) Quartz**

The quantity of quartz varies between 30-50%. Crystals are anhedral and tend to have serrated boundaries. The size of quartz crystals is variable but tends to range between 0.02 and 0.04 mm in massive rhyodacites and between 0.03 and 0.08 mm in flow banded rhyolites. Local phenocrysts average about 0.12 mm in length. Quartz bands in flow-banded rhyolites are between 0.04 and 0.1 mm thick.

#### **(4.2.12) K-Feldspar**

Percentages of K-feldspar range from 33-45%. Crystals are anhedral with serrated boundaries. Sizes of groundmass K-feldspar crystals in both massive and flow banded samples average between 0.01 and 0.04 mm whereas phenocrysts are between 0.20 and 0.97 mm. K-feldspars have a slightly “dirty” appearance as they are less pristine than quartz crystals and undergoing minor sericitization.

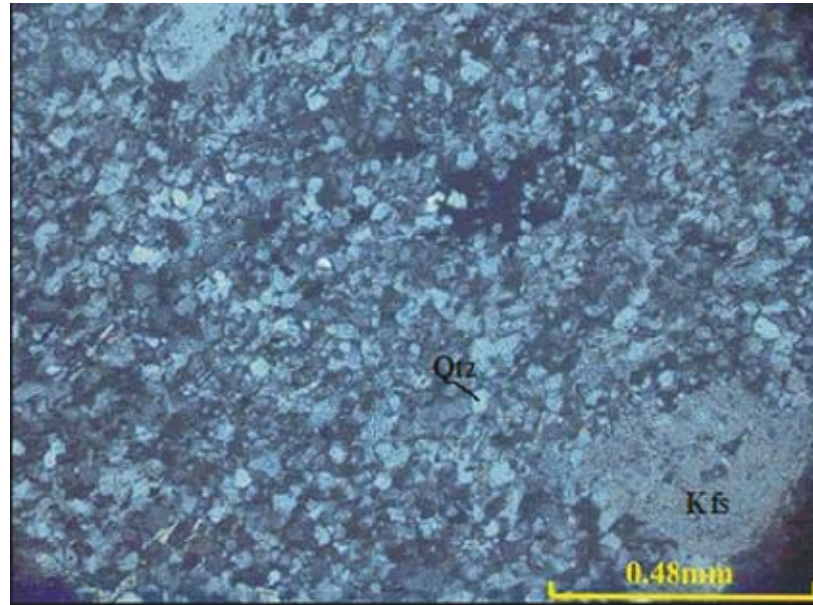


Figure 17: Photograph of sample 05NB-07-1 showing the typical petrographical characteristics of massive Kitselas rhyolites at 10x magnification with crossed polars. K-feldspars tend to be less pristine than quartz crystals and are undergoing minor sericitization.

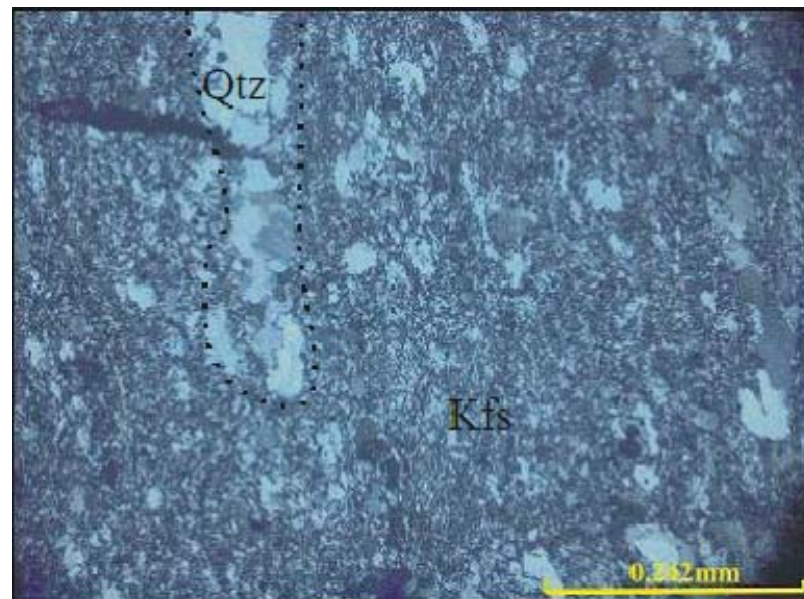


Figure 18: Sample 05NB-26-3 is a flow-banded rhyolite from Kitselas Mountain; it is composed of thick layers of fine-grained potassium feldspar and thin layers of quartz crystals. An example of a quartz band is outlined with a dotted line. This photograph was taken at 20x magnification with crossed nicols.

#### **(4.2.13) Plagioclase**

Rare plagioclase occurs as phenocrysts and as part of the groundmass in the felsic Kitselas samples. Crystals are subhedral, lath shaped, and undergoing minor sericitization and grain sizes are similar to those of quartz and K-feldspar crystals.

#### **(4.3) Telkwa Andesites and Basalts**

Of the five mafic Telkwa samples, two are basalts (05NB-31-1 and 05NB-03-6) and three are andesites (05NB-01-1, 05NB-15-5, and 05NB-16-3). A plagioclase, pyroxene, +/- quartz assemblage characterizes mafic rocks of the Telkwa Formation. They have a variety of textures including aphyric, porphyritic, seriate, amygdaloidal, trachytic, pilotaxitic, and poikilitic. Common forms of alteration include sericitization, chloritization, saussuritization, uralitization, and carbonitization.

##### **(4.3.1) Mineralogy and Textures**

###### **(4.3.11) Plagioclase**

Plagioclase accounts for approximately 45 to 80% volume of the mafic Telkwa samples. Crystal sizes are variable; they range from 0.04 to 0.15 mm where part of the groundmass whereas phenocrysts are between 0.13 to 0.51 mm. Phenocryst concentration is relatively low, accounting for only a maximum of about 5% of plagioclase grains. Crystals are locally aligned, typically subhedral to euhedral, and elongate to lath shaped. Although plagioclase is often altered, crystal boundaries are usually well defined and primary textures are well preserved. The most common type of alteration of plagioclase crystals is minor sericitization; this has occurred in almost all of the samples. The alteration of plagioclase to calcite is also common; this occurs in half of the samples leaving calcite to account for up to approximately 17% of the mineralogy. Minor

saussuritization was observed in sample 05NB-15-5. Propylitization affected the plagioclase grains in sample 05TB-31-1, leaving a mix of chlorite, epidote, and albite at the centre of crystals and along cleavage plains and fractures (figure 19). Plagioclase crystals locally contain rare small inclusions of anhedral epidote; the original composition of these inclusions was likely pyroxene.

#### **(4.3.12) Clinopyroxene**

Clinopyroxene concentrations are variable in mafic rocks of the Telkwa Formation accounting for anywhere from 0 to approximately 40 % of the mineralogy. Most crystals are in the groundmass but rare phenocrysts are also present. Clinopyroxenes are anhedral to euhedral, however, crystal form is often masked by alteration; epidote is the major alteration product of clinopyroxene. An eight sided crystal shape can be seen when epidote pseudomorphs clinopyroxene grains; this most often occurs in phenocrysts (figure 20). Uralitization is also fairly common as pyroxene grains are altering to metamorphic actinolite in three of the five samples; primary textures may or may not be preserved. In one sample (05TB-31-1), actinolite follows cleavage planes giving a very fibrous texture to clinopyroxene crystals (figure 21). Chloritization of clinopyroxene is also common.

#### **(4.3.13) Quartz**

Quartz is a minor component of the groundmass in samples 05NB-15-5 and 05NB-16-3 and it comprises up to 10% of the mineralogy. Anhedral crystals have irregular to serrated boundaries and are generally between 0.04 and 0.06 mm.

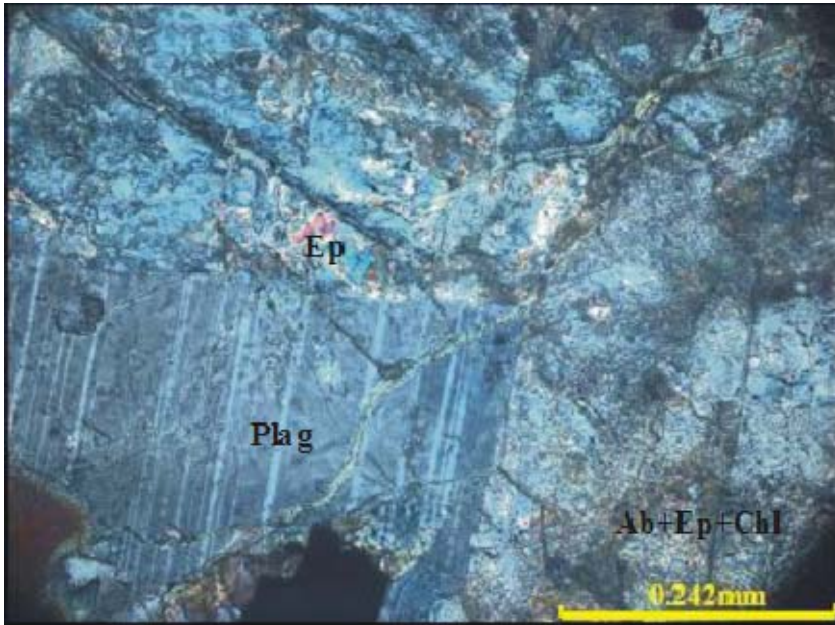


Figure 19: Propylitization results in the alteration of plagioclase to a mixture of epidote, albite, and chlorite in sample 05TB31-1. The photograph was taken at 20x magnification with crossed nicols.

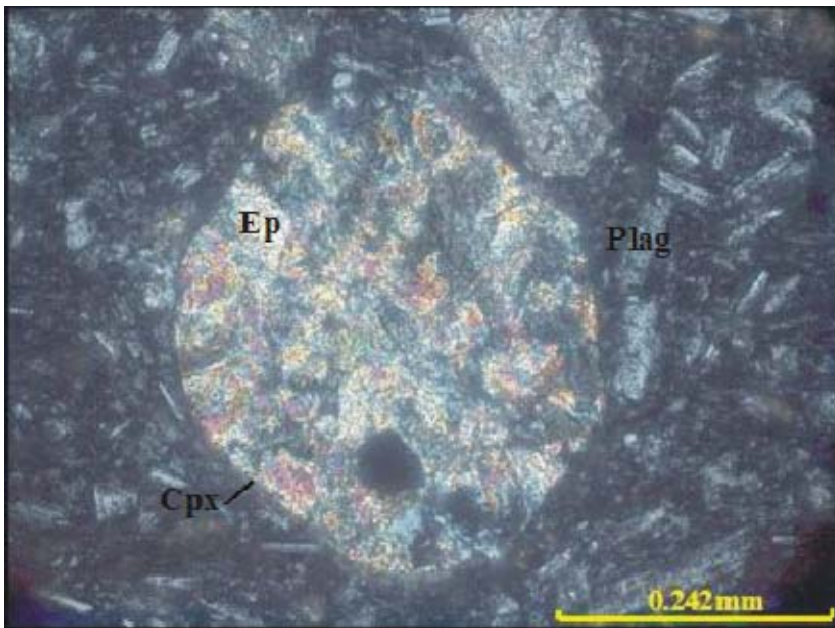


Figure 20: Epidote pseudomorphs the crystal form of pyroxene in sample 05NB15-5. The photograph was taken at 20x magnification with crossed nicols.

#### **(4.3.14) Composition of Lapilli**

Sample 05NB-16-3 was taken from an andesitic lapilli tuff on the highway between Kleanza and Chindemash Creeks. Lapilli in this sample are composed of plagioclase, clinopyroxene, and quartz; they appear to be slightly coarser grained autoclasts. Alteration patterns of these fragments are identical to those seen in the groundmass of this sample.

#### **(4.3.15) Secondary Minerals**

Sericite frequently replaces plagioclase grains; crystals tend to be fibrous to platy but are also anhedral. Percentages of sericite range between 1 and 5%. The one lapilli tuff, however, contains two to three times that amount; this trend is typical of this sample, as it also contains higher than normal amounts of actinolite and epidote. The most common ferromagnesian alteration minerals in these Telkwa rocks are epidote and chlorite. Epidote often forms anhedral aggregates and accounts for anywhere from 0 to 30% of rock volumes. Anhedral to fibrous chlorite is much less common and comprises only up to 7% volume. Actinolite, where present, is fairly abundant averaging about 10% of the mineralogy. Crystals are elongated, bladed, and acicular (figure 22). Calcite is anhedral, replaces plagioclase crystals, and together with epidote, chlorite, and actinolite forms scarce veinlets and amygdules. Red to brown iron oxide is present in the groundmass of two samples; it occupies about 10% of the rock volume in sample 05NB-01-1 and 3% in sample 05NB-22-4.

#### **(4.4) Telkwa Rhyolites**

Samples 05NB-23-2, 05NB-39-9, and 05NB-33-1 are Telkwa rhyolites. Two of these samples are massive (05NB-23-2 and 05TB-39-9) (figure 23) and the other is flow

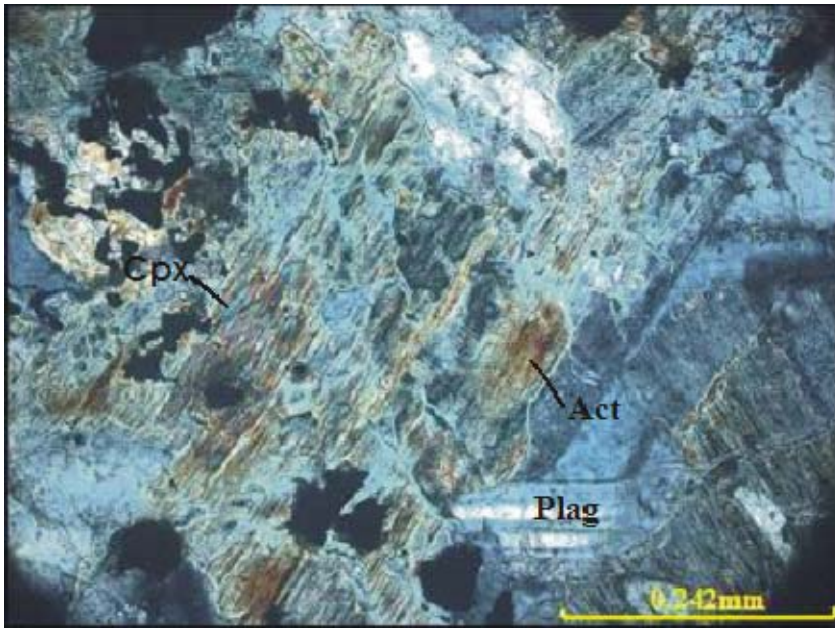


Figure 21: Actinolite concentrates along the cleavage planes of clinopyroxene grains in sample 05TB31-1 leaving them with a fibrous texture. The photograph was taken at 20x magnification with crossed nicols.

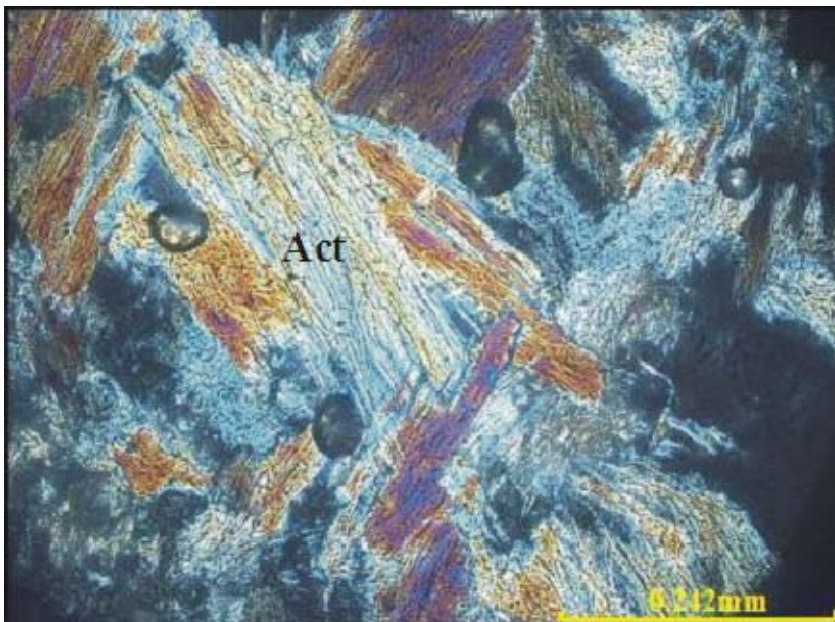


Figure 22: The presence of actinolite in some of the Telkwa andesites and basalts is suggestive of greenschist metamorphic grade. This is a photograph of actinolite in sample 05NB-03-1 taken at 20x magnification with crossed nicols.

banded and amygdaloidal (05TB-33-1). These three samples are composed of quartz, potassium feldspar, and +/- minor plagioclase. Where present, plagioclase phenocrysts account for approximately half of all plagioclase crystals.

#### **(4.4.1) Mineralogy and Textures**

##### **(4.4.11) Quartz**

Quartz is the predominant mineral in the flow banded sample and accounts for approximately 60% of the rock volume. This mineral only accounts for up to 30% of the rock volume in massive samples. Crystals are anhedral with irregular to serrated boundaries. Crystal sizes are variable and range from 0.03 to 0.1 mm in massive rocks and from 0.02 to 0.06 mm in flow banded rocks. Quartz crystals of different sizes are separated into layers in the flow-banded sample.

##### **(4.4.12) K-feldspar**

Potassium feldspar is the dominant mineral in massive samples; it accounts for 55-65% of the mineralogy in massive rhyolites whereas it occupies only about 25% of the rock volume in the flow-banded sample. Crystal sizes and the nature of their boundaries are difficult to determine as most crystals are undergoing alteration to sericite. Surfaces tend to have a chewed to dirty appearance as they are less pristine than quartz grains.

##### **(4.4.13) Plagioclase**

Plagioclase occurs in massive samples as both part of the groundmass and as scarce phenocrysts and accounts for 5 to 15% of the volume. Crystals range from 0.08 to 0.2 mm in groundmasses whereas phenocrysts are between 0.5 and 1.3 mm. Plagioclases are elongated to lath shaped and boundaries tend to be relatively well defined. Minor sericitization affects plagioclase grains.

**(4.4.14) Clasts**

Sample 05NB-23-2 also contains a very small amount (1%) of felsic clasts. These clasts tend to be sub-rounded and are composed of either potassium feldspar and quartz or a mass of plagioclase crystals. Minerals in these clasts share very similar textures to those that comprise the groundmass; these clasts are likely autoliths and/or xenoliths.

**(4.4.15) Secondary Minerals**

Sericite replaces K-feldspar and plagioclase in all samples and accounts for 5 to 20 % of the mineralogy. Crystals are anhedral, platy, and fibrous and locally form stockworks throughout the groundmass. Amygdules are filled with quartz, sericite, epidote, amphibole (likely hornblende), and chlorite.

**(4.5) Intermediate Telkwa Sample**

Sample 05NB-23-4 is dacitic in composition. Euhedral to subhedral plagioclase crystals make up most of the groundmass, although they also occur as rare phenocrysts. The groundmass has a trachytic texture and this sample is amygdaloidal. Common forms of alteration are minor sericitization and carbonitization.

**(4.6) Mount Pardek Sample**

The Mount Pardek sample (05TB-25-3) is volcanoclastic and is characterized by felsic xenoliths and/or lapilli engulfed in a more mafic body; these lapilli and xenoliths make up about 15% of the sample. Primary minerals and textures are very difficult to identify as mafic portions of this sample are highly altered (figure 24). In general, the groundmass of this sample is predominantly composed of plagioclase and pyroxene. Crystal sizes are obscured, however, both plagioclase and pyroxene occur as part of the groundmass and as phenocrysts. Sericitization of plagioclase is common as sericite

accounts for up to 15% of the slide. Pyroxene is altered to chlorite, epidote, and actinolite; these secondary minerals have similar habits and textures to those found in other Kitselas and Telkwa rocks. Felsic lapilli and/or xenoliths are well rounded to subangular and composed of quartz and rhyolite fragments. Reaction rims around some of these lithics are indicative of disequilibria (figure 25).

## **(5.0) Geochemistry**

### **(5.1) Experimental Methods**

Geochemical classification and comparison of Telkwa and Kitselas rocks was used to help determine the primary relationship between the two units. Fifteen samples of volcanic rocks, which are representative of variations in the map sheet, were analysed; of these, 6 are Kitselas volcanics (05NB-07-1, 05NB-26-1, 05NB-26-3, 05NB-28-1, 05NB-28-2, and 05NB-29-2) and the remaining 9 are from the Telkwa Formation (05NB-01-1, 05NB-03-6, 05NB-15-5, 05NB-23-2, 05NB-23-4, 05TB-25-3, 05NB-31-1, 05NB-33-1, and 05NB-39-9). In all cases, care was taken in choosing massive, homogeneous, unveined, non-amygdaloidal, and least altered samples. In situations where rare veinlets and amygdules were unavoidable, they were removed from the sample before analysis. Major and some trace element ( $\text{SiO}_2$ ,  $\text{TiO}_2$ ,  $\text{Al}_2\text{O}_3$ ,  $\text{Fe}_2\text{O}_3$ ,  $\text{MnO}$ ,  $\text{MgO}$ ,  $\text{CaO}$ ,  $\text{Na}_2\text{O}$ ,  $\text{K}_2\text{O}$ ,  $\text{P}_2\text{O}_5$ , V, Cr, Co, Zr, Ba, La, Nd, Ni, Cu, Zn, Ga, Rb, Sr, Y, Nb, Pb, Th, and U) compositions were determined at the Saint Mary's University Geochemical Centre with the use of x-ray fluorescence spectrometry. The spectrometer used for the analysis was the Philips PW2400. REE and trace element data (Y, Zr, Nb, La, Ce, Pr, Nd, Sm, Eu, Gd, Tb, Dy, Ho, Er, Tm, Yb, Lu, Hf, Ta, and Th) were acquired from Memorial University

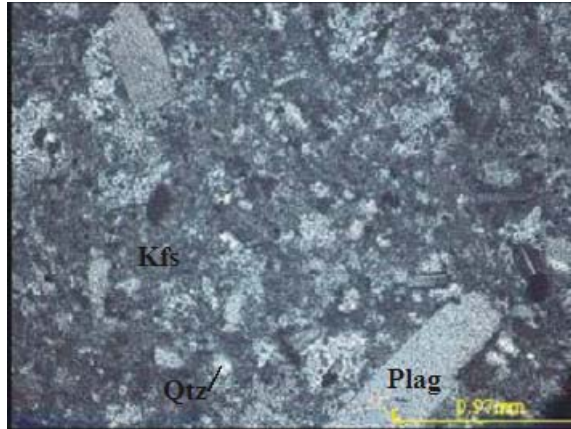


Figure 23: A photograph of sample 05NB-23-2 at 5x magnification and with crossed polars showing the typical petrographical characteristics of massive Telkwa rhyolites.

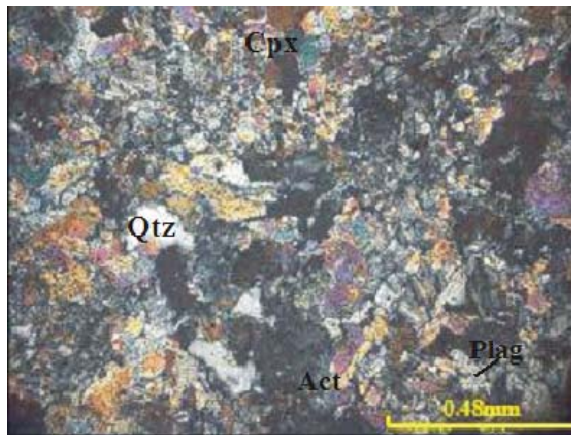


Figure 24: Typical petrographical characteristics of the Mt Pardek sample (05TB-25-3). The photograph was taken with crossed nicols at 10x magnification.

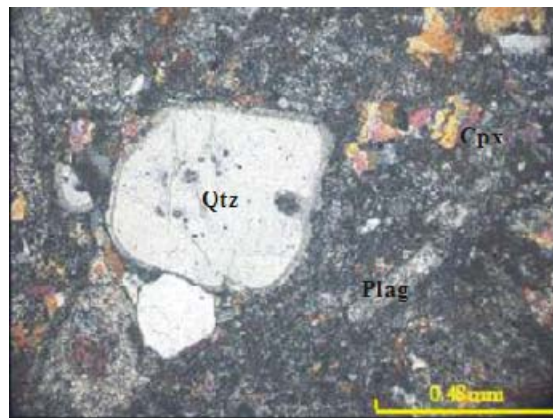


Figure 25: A Reaction rim around a quartz crystal in sample 05TB-25-3 indicates conditions of disequilibria. The photograph was taken with crossed nicols at 10x magnification.

using inductively coupled mass spectrometry (model VG PQ2+S). Results from Memorial University were preferentially used over those from Saint Mary's University whenever possible due to the higher detection limit of ICPMS. All geochemical data are presented in tables A-1, A-2, and A-3.

### **(5.2) Post-Magmatic Alteration**

High "loss on ignition" values are indicative of post-magmatic alteration. Although an attempt was made to avoid sampling altered rocks, L.O.I values for this suite range between 0.20 wt % and 6.06 wt % with an average value of 2.38 wt %. These values suggest that some of the rocks from both the Telkwa Formation and Kitselas volcanic sequence have undergone alteration. Certain elements, especially alkali earth metals, become mobilized under these conditions and are thus unreliable for the characterization of these rocks (Bailes et al., 1996). High Field Strength Elements (Ti, Zr, Hf, Nb, Ta, P, Y), which are small highly charged cations, and Rare Earth Elements (La, Ce, Pr, Nd, Pm, Sm, Eu, Gd, Tb, Dy, Ho, Er, Tm, Yb, and Lu) are thought to remain mostly immobile under normal conditions of alteration and during low-grade metamorphism (Bailes et al., 1996); therefore, whenever possible, classification of Telkwa and Kitselas rocks was conducted using silica, HFSE's, and REE's.

### **(5.3) Rock Type Classification**

Volcanic rocks from both the Telkwa Formation and the Kitselas volcanic sequence span a compositional range from basalts (50.05 wt% SiO<sub>2</sub>) to high silica rhyolites (79.34 wt% SiO<sub>2</sub>) or from andesitic basalts to rhyolites depending on the discrimination diagram used for their classification. Trace element diagrams rely on the fact that immobile elements and their ratios vary in a distinct fashion as magmas evolve;

their concentrations and ratios can therefore be used to characterize different rock types of different series. The word series refers to a group of rocks that share similar chemical, and often mineralogical, characteristics resulting from a genetic relationship (Winter, 2001). Iddings (1892) proposed that all igneous rocks belong to either the sub-alkaline or alkaline series (Winter, 2001). In the Winchester and Floyd diagram (1976) (figure 26),  $Zr/TiO_2$  ratios are used to distinguish between the alkaline and subalkaline series, the latter of which tends to undergo a greater degree of differentiation.  $Zr/TiO_2$  ratios increase as magmas evolve. Ti is highly incompatible (meaning that it prefers the melt phase) in basaltic magmas but becomes compatible during the fractional crystallization of intermediate to acidic magmas. More evolved melts will therefore show an overall decrease in Ti concentrations. Zr on the hand remains incompatible during fractional crystallization up to intermediate-acidic compositions. The increase in  $Zr/TiO_2$  in comparison to the increase in Si concentrations can therefore be used as a measure of alkalinity (Winchester and Floyd, 1976). Also, Zr concentrations tend to be much higher in alkaline basalts contributing to the more inclined nature of alkaline trend lines on this diagram (Winchester and Floyd, 1976). One problem with the use of this diagram for this project is that Si is sometimes mobile. Thus, this variable may not be entirely reliable for accurately determining the degree of differentiation in altered samples. Another option would be to analyze the data with a diagram that utilizes immobile elements only.

In the Winchester and Floyd (1976)  $Zr/TiO_2$ -Nb/Y diagram (figure 27), both  $Zr/TiO_2$  and Nb/Y ratios are used as a measure of alkalinity, whereas only  $Zr/TiO_2$  ratios are used to represent degrees of differentiation (Winchester and Floyd, 1976). Nb values tend to be characteristically lower in sub-alkaline suites than in alkaline suites (see

sections ahead). Higher Nb/Y ratios, therefore, generally tend to represent the alkaline suite, whereas Zr/TiO<sub>2</sub> ratios increase from basaltic to rhyolitic compositions (Winchester and Floyd, 1976).

Rocks from both the Telkwa Formation and the Kitselas volcanic sequence define a sub-alkaline trend. Samples are widely distributed in their composition when plotted on the SiO<sub>2</sub>-Zr/TiO<sub>2</sub> diagram whereas they tend to “clump” together when plotted on the Zr/TiO<sub>2</sub>-Nb/Y diagram. It is unlikely that this discrepancy is due to the mobilization of silica since the quartz in these samples was determined to be almost entirely primary upon petrographic analysis. It is not uncommon to see differences between diagrams simply due to natural variations in the chemical compositions of igneous rocks as compared to those used to construct these diagrams (Rollinson, 1993). In any case, the difference in composition of any one sample between diagrams tends to be minor; for example, the difference between a basalt and an andesitic basalt. For the purpose of this thesis, we will classify the samples using the SiO<sub>2</sub>-Zr/TiO<sub>2</sub> diagram because its results parallel the petrographic classification.

## **(6.0) Discussion**

### **(6.1) Basalt Classification**

The ratios in both the Winchester and Floyd (1976) SiO<sub>2</sub> vs. Zr/TiO<sub>2</sub> and the Winchester and Floyd (1976) Zr/TiO<sub>2</sub> vs. Nb/Y diagrams suggest that the samples belong to the sub-alkaline series. Igneous rocks of the sub-alkaline series may belong to either the tholeiitic or calc-alkaline series; therefore, further classification of these samples was done using the AFM Irvine and Baragar (1971) and Miyashiro (1974) diagrams (figures

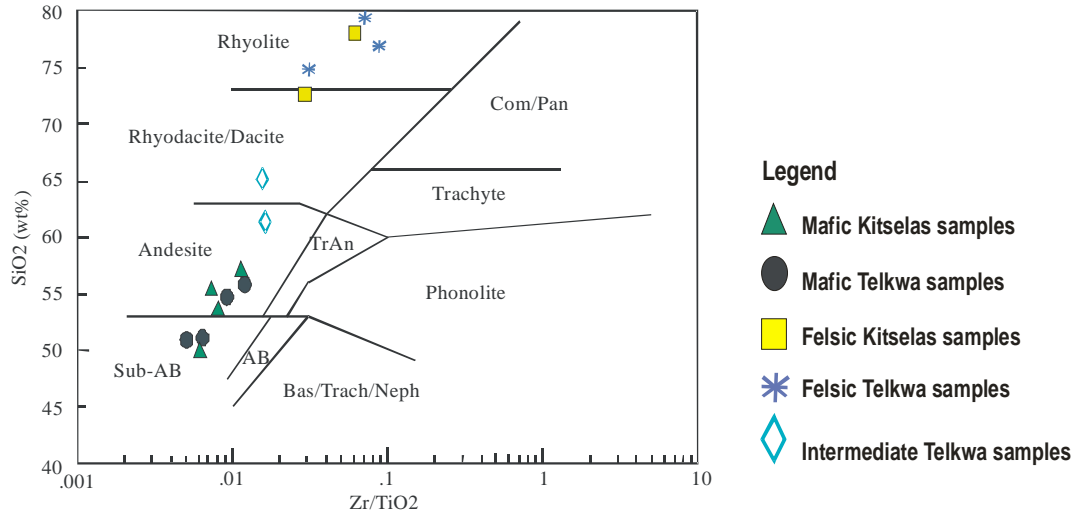


Figure 26: Rocks from both the Telkwa Formation and the Kitselas volcanic sequence define a sub-alkaline trend when Si concentrations are used in their classification. Diagram from Winchester and Floyd, 1976.

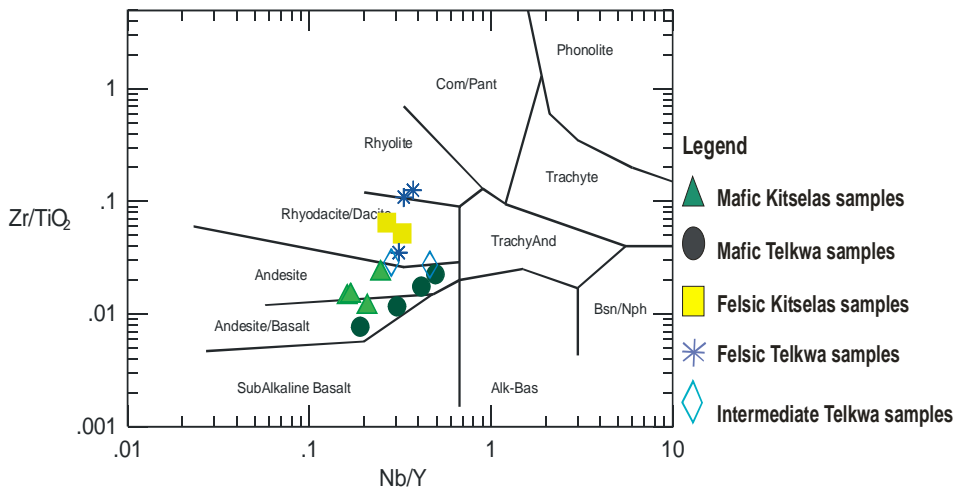


Figure 27: Rocks of the Telkwa Formation and the Kitselas volcanic sequence define a sub-alkaline trend when only trace element concentrations are plotted. Diagram from Winchester and Floyd, 1976.

28 and 29 respectively) (Winter, 2001). The AFM diagram subdivides calc-alkaline and tholeiitic basalts according to the pattern of iron enrichment. Tholeiitic magmas are

characterized by strong iron enrichment in comparison to magnesium at lower concentrations of  $K_2O + Na_2O$ . Calc-alkaline basalts may show this pattern to a lesser degree or not at all (Winter, 2001). Tholeiitic volcanic rocks characteristically contain a higher percentage of ferromagnesian minerals than rocks of the calc-alkaline suite. Magnesium is preferentially incorporated into the lattice of ferromagnesian minerals at greater depths and temperatures enriching the melt in iron during earlier stages of crystallization (Winter, 2001). More importantly, calc-alkaline magmas are thought to be generated in conditions where oxygen fugacity is relatively high. This may be due to a larger amount of water being incorporated into the mantle from the subducting slab as the system progresses. The generation of new melts becomes increasingly difficult with time as peridotites in the mantle wedge become depleted in their basaltic components; they will thus require greater amounts of water to induce partial melting (Miyashiro, 1974). Iron may then be oxidized and precipitated out of the system under these conditions. In addition to this pattern of iron enrichment, the  $TiO_2$  vs.  $FeO^*/MgO$  diagram also utilizes

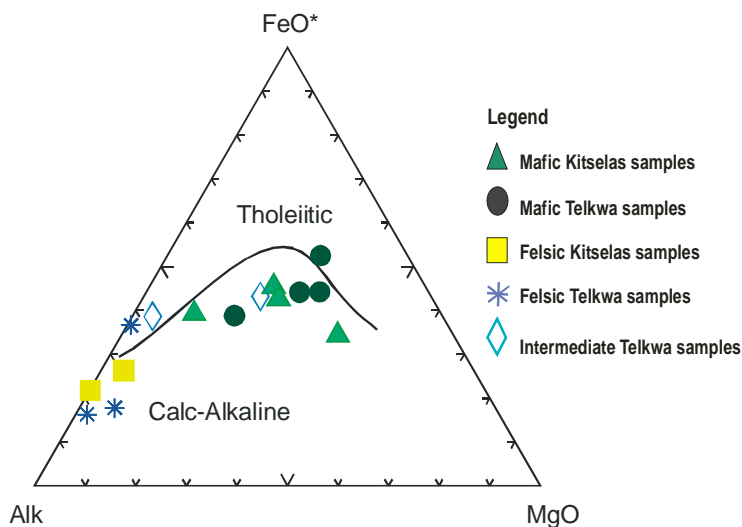


Figure 28: Plotting the data on an AFM diagram indicates that rocks from both the Kitselas volcanic sequence and the Telkwa Formation are part of a calc-alkaline suite. Diagram from Irvine and Baragar, 1971.

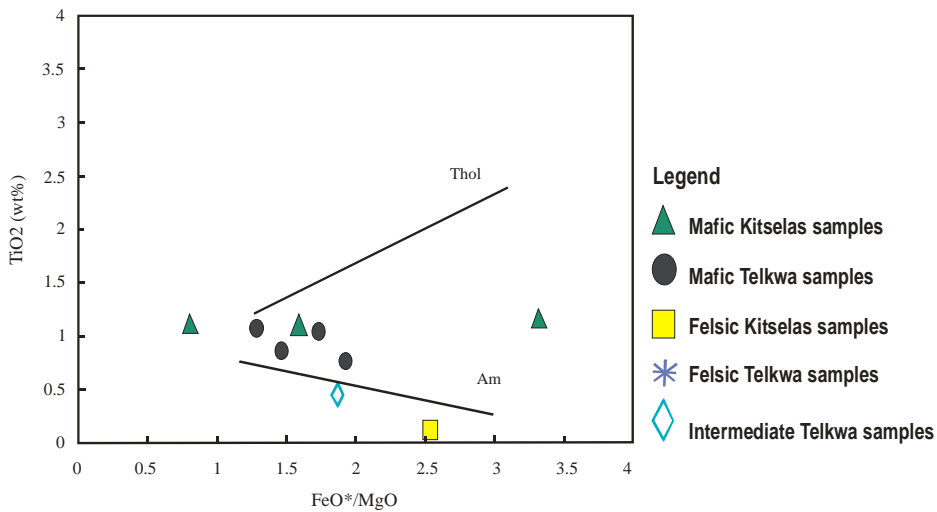


Figure 29: Rocks of the Telkwa Formation and of the Kitselas volcanic sequence define a calc-alkaline trend when  $\text{FeO}^*/\text{MgO}$  ratios and  $\text{TiO}_2$  concentrations are plotted on the Miyashiro (1974) diagram.

trends observed in  $\text{TiO}_2$  to distinguish between tholeiitic and calc-alkaline basalts.  $\text{TiO}_2$  concentrations will decrease with decreasing  $\text{FeO}^*/\text{MgO}$  ratios in calc-alkaline basalts but will increase and then decrease in the tholeiitic sequence (Miyashiro, 1974). The trend in  $\text{TiO}_2$  concentrations thus seems to parallel that of  $\text{FeO}^*$ . One reason for this may be due to the early crystallization of magnetite under oxidizing conditions, as substantial amounts of Ti may be incorporated into the lattice of this mineral; titaniferous magnetite would likely only crystallize in later stages under reducing conditions (Miyashiro, 1974). The Telkwa and Kitselas andesitic and basaltic samples clearly define a calc-alkaline trend in both diagrams.

### (6.2) Determining the Tectonic Setting using Discrimination Diagrams

If rocks from both the Telkwa Formation and the Kitselas volcanic sequence are genetically related, both suites must come from a similar tectonic setting. Rocks of the Telkwa Formation have previously been determined to be of island arc origin, thus one

may postulate that rocks chosen for this analysis are part of an island arc suite. Island arc volcanics are generated along destructive plate margins. Partial melting of the subducting basaltic ocean crust may be initiated by the dehydration of the subducting slab (Winter, 2001). The partial melts derived from the former oceanic crust become enriched in incompatible elements. They then migrate upwards into the overlying depleted peridotite mantle where hybridization of the two magmas leads to an enriched mantle source region for island arc magmas (Ringwood, 1989). Rocks of the calc-alkaline series, which are the dominant series in island arc settings, typically display a strong enrichment of low field strength elements (large ionic radius, weakly charged, and most incompatible) in comparison to high field strength elements (Bailes et al., 1996). This effect is also partially attributed to the relatively low and high solubilities of HFSE and LFSE respectively (Ringwood, 1989).

To help determine the tectonic setting of the andesites and basalts, their chemistry was plotted on the Ti/100-Zr-Y\*3 trace element discrimination diagram by Pearce and Cann (1973) (figure 30) and on the Th-Ta-Hf diagram by Wood et al. (1979) (figure 31). The first of these diagrams best distinguishes between within plate basalts (WPB) and other magma types, whereas the mid-ocean ridge basalt (MORB) and volcanic arc basalt (VAB) fields tend to overlap one another to a noteworthy degree (Bailes et al., 1996). Separation of WPB magma types from other types on this diagram is mainly influenced by Y concentrations, as WPB tend to be depleted in this element. Lavas that are transitional in specific tectonic environments primarily cause discrepancies between the MORB and VAB fields (Bailes et al., 1996). Overlap between these fields often occurs in marginal basins, where high degrees of melting of a highly depleted mantle source are

generated by the combination of water in the mantle and by decompression beneath the arc. However, degrees of crustal assimilation are considerably less than those in a typical island arc, leading to the more primitive composition of back arc basalts (Bailes et al., 1996). Mafic to intermediate samples from both the Telkwa Formation and the Kitselas volcanic sequence plot in fields B and C on the Ti/100-Zr-Y\*3 diagram, thus defining a calc-alkaline trend with some uncertainty.

The Th-Ta-Hf diagram best discriminates between VAB and other magma types whereas the MORB and WPB fields overlap to a significant degree. Here again, volcanics generated in transitional settings are the main cause for overlap (Bailes et al., 1996). The element Th acts as the main discriminant between arc basalts and other magma types. Calc-alkaline basalts (which plot in the lower left portion of the VAB field) will be particularly enriched in this element, since the majority of Th resides in the upper continental crust and these volcanics are believed to undergo higher amounts of

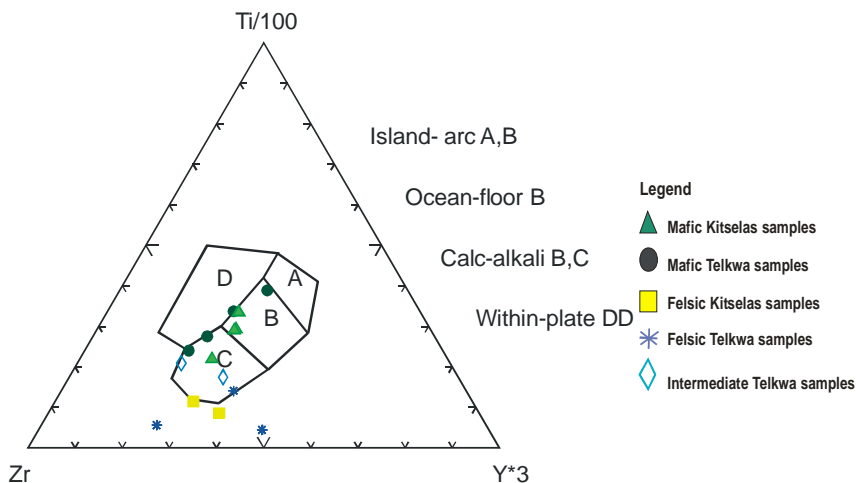


Figure 30: The Telkwa and Kitselas samples plot in fields B and C thus suggesting that they are part of a calc-alkaline suite. Diagram from Pearce and Cann, 1973.

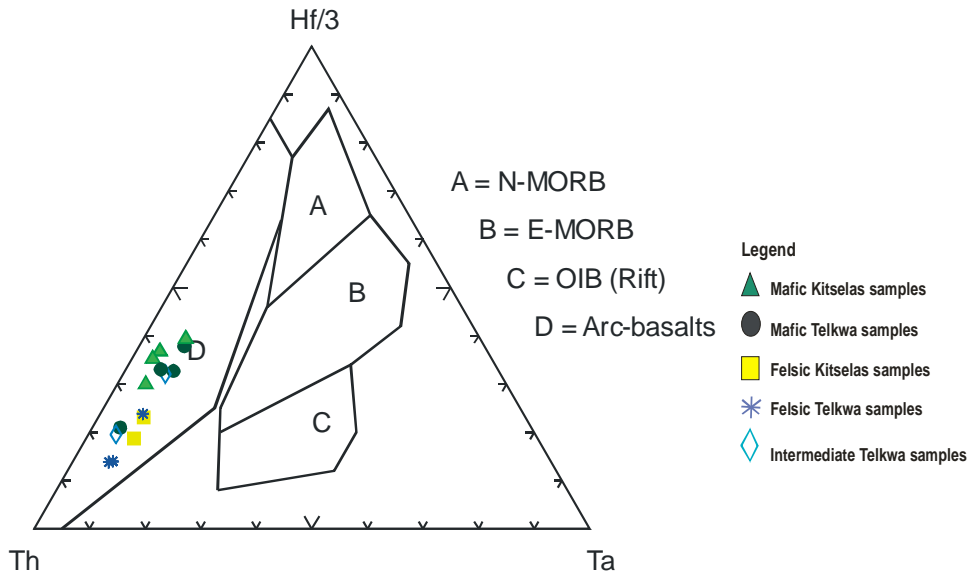


Figure 31: All samples clearly plot in field D indicating that they have been derived from an island arc volcanic setting. Diagram from Wood et al, 1979.

crustal assimilation (Bailes et al., 1996). All samples from both the Telkwa and Kitselas suites clearly plot in the calc-alkaline VAB field in this diagram.

### (6.3) Normalized Trace Element Diagrams

Normalized trace element plots measure the deviations in trace element chemistry from a chondrite, primitive mantle, or normal mid-ocean ridge basalt depending on the diagram used. These diagrams are useful as deviation patterns often reflect the tectonic origin(s) of the samples in question. Element concentrations are plotted on a log scale; a value of one acts as a reference for a chondrite, primitive mantle, or average MORB (Bailes et al., 1996). Normalized MORB diagrams were chosen for trace element analysis in this project. Elements on the x-axis of an N-MORB Sun and McDonough (1989) spider diagram are arranged in order of increasing compatibility with respect to a small amount of peridotitic mantle melt that would give rise to a normal mid-ocean ridge basalt (Bailes et al., 1996).

### **(6.3.1) Interpreting Trace Element Patterns**

A normal (N)-type MORB will plot as a fairly smooth curve at, or very close to, a value of one (because the sample is of the same rock type as the reference rock).

Enriched (E)-type mid-ocean ridge basalts also plot as a smooth curve but with a slight enrichment in the more incompatible elements. The pattern of enrichment in (E)-type MORBs is thought to be the result of a deep enriched mantle source (Winter, 2001). Similar patterns are observed in ocean island basalts although they tend to be slightly more enriched than E-MORBs; OIBs are thus thought to also originate from a lower enriched mantle reservoir (Winter, 2001).

Volcanic arc rocks typically show an enrichment of LFSE relative to HFSE for reasons described above. The most diagnostic trend of these rocks is an anomalous depletion in niobium, tantalum, and titanium. The Ti may be residing in a residual rutile bearing quartz free eclogite (Ringwood 1989). Niobium and tantalum are strongly partitioned into rutile at depths and temperatures appropriate for the melting of a subducting slab (Ringwood 1989).

Rocks derived from intraplate magmas generally tend to show similar trends to those of arc basalts but without the strong negative Nb, Ta and Ti anomalies. It has been postulated that the production of intraplate magma is an extension of the processes responsible for the formation of island arc volcanics accounting for these similarities in trace element chemistry. The lack of Nb, Ta, and Ti anomalies in intraplate volcanics may be attributed to the lack of stability of rutile at greater depths as the subducting slab progresses; these elements would then become highly incompatible and shift to the melt phase (Ringwood, 1989).

### (6.3.2) Trace Element Patterns of the Telkwa and Kitselas Volcanic Rocks

#### (6.3.2.1) Tectonic Implications

The mafic, intermediate, and felsic samples of the Telkwa Formation and Kitselas volcanic sequence show trace element patterns typical of volcanic arc derived rocks (figures 32, 33, and 34 respectively). Firstly, these rocks show a prominent enrichment of LFSE as compared to HFSE when plotted on normative diagrams. This pattern of enrichment rules out the possibility that the Telkwa and Kitselas samples are normal mid-ocean ridge basalts, as N-type MORBs should plot as a smooth curve close to a value of one. Secondly, because other types of igneous rocks (e.g. E-MORB, OIB, etc.) are also enriched in LFSE, it is important to refer to the Nb values before drawing any further

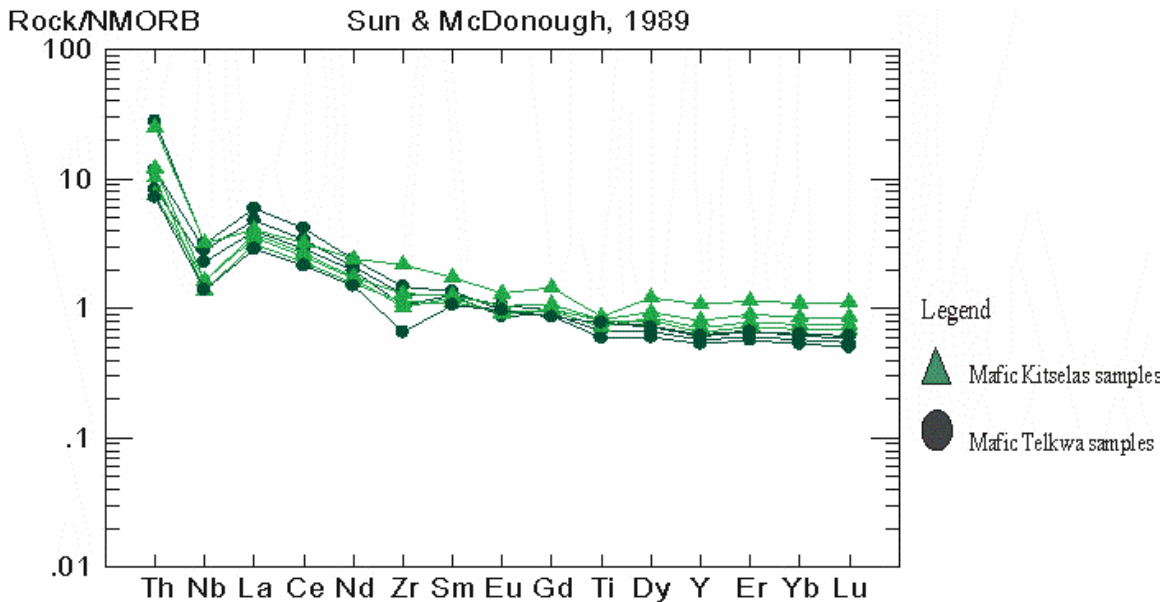


Figure 32: Trace element patterns for the Telkwa and Kitselas volcanic rocks show enrichment in LFSE's, Nb depletions, and share very similar characteristics. Diagram and normalizing values from Sun and McDonough, 1989.

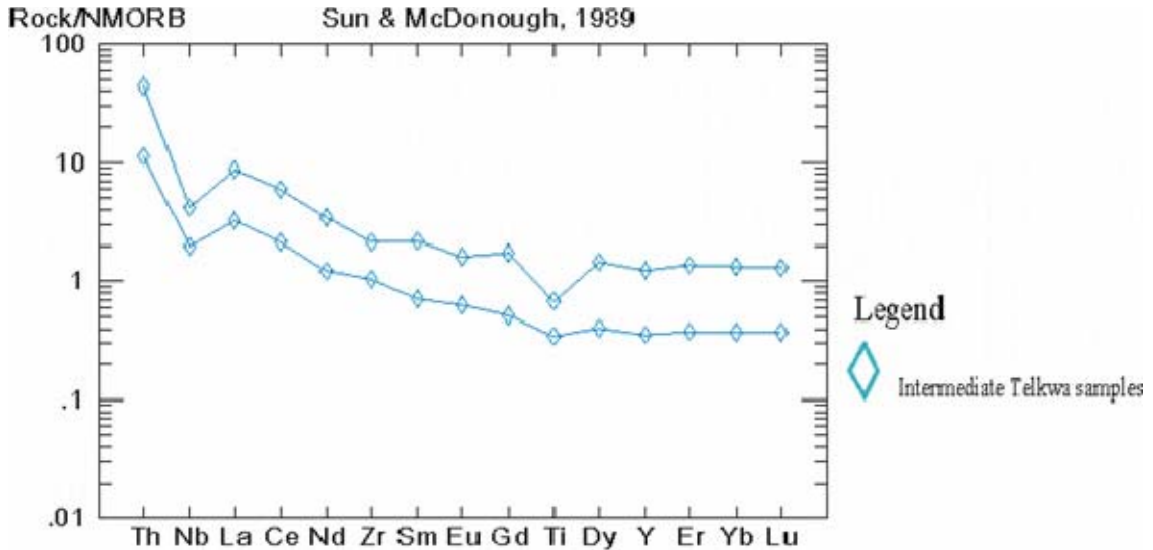


Figure 33: Intermediate samples define a subduction related trend. Diagram and normalizing values from Sun and McDonough, 1989.

conclusions. All of the samples analyzed in this experiment show anomalous Nb depletions characteristic of island arc basalts, thus supporting the theory that they have originated from an arc environment.

### (6.3.22) Primary Relationship of Telkwa and Kitselas Samples

Unrelated volcanic suites are typically represented by scattered data and enrichment depletion patterns distinct from one another. Mafic rocks from the Kitselas volcanic sequence and Telkwa Formation share very similar chemical trends thus suggesting that these two map units are genetically related (figure 32). Similar patterns are observed within the felsic Kitselas and Telkwa samples (figure 34).

All samples were plotted on one normalized trace element diagram to analyse the relationship between felsic and mafic Kitselas and Telkwa rocks (figure 35). The resulting pattern shows a continuous increase in the concentrations of the most incompatible elements and a strong decrease in Ti values in felsic samples. These results

again suggest a genetic relationship; as a magma continues to evolve, the most incompatible elements will be forced to crystallize from the melt, and thus their concentrations should become progressively higher in more felsic suites. Ti concentrations should decrease with the evolution of a melt for reasons discussed in the Rock Type Classification section.

An interesting difference in trace element patterns between the two units is the slight enrichment of the most compatible elements in the Kitselas volcanic sequence. This pattern is most obvious in the more mafic samples and may suggest that the Kitselas rocks were formed slightly earlier than the Telkwa rocks, as these elements would begin crystallizing from a melt first (figure 32).

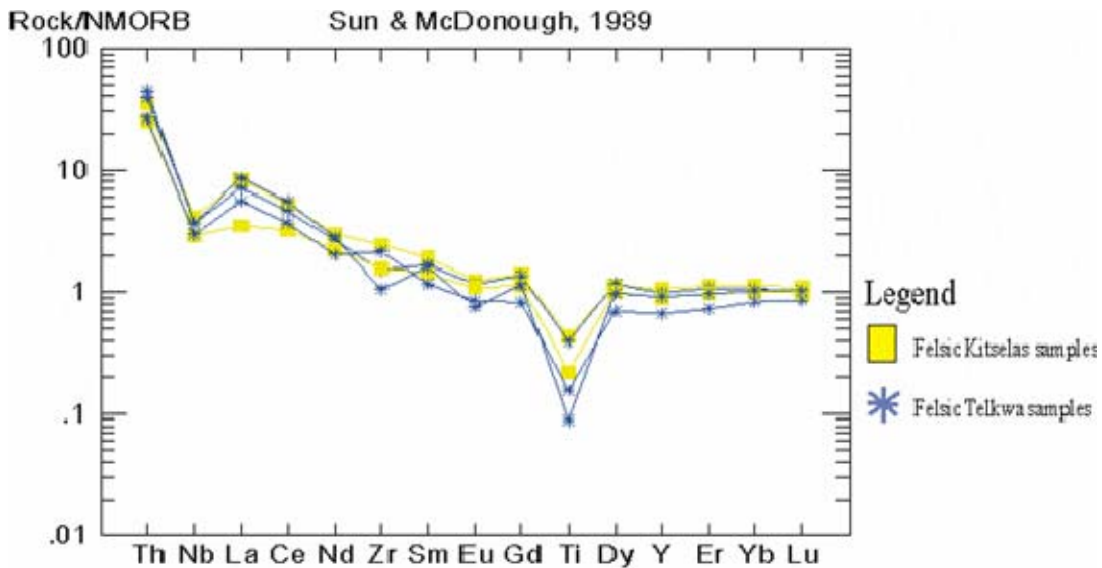


Figure 34: Felsic Telkwa and Kitselas samples define a subduction related trend and share very similar trace element characteristics. Diagram and normalizing values from Sun and McDonough, 1989.

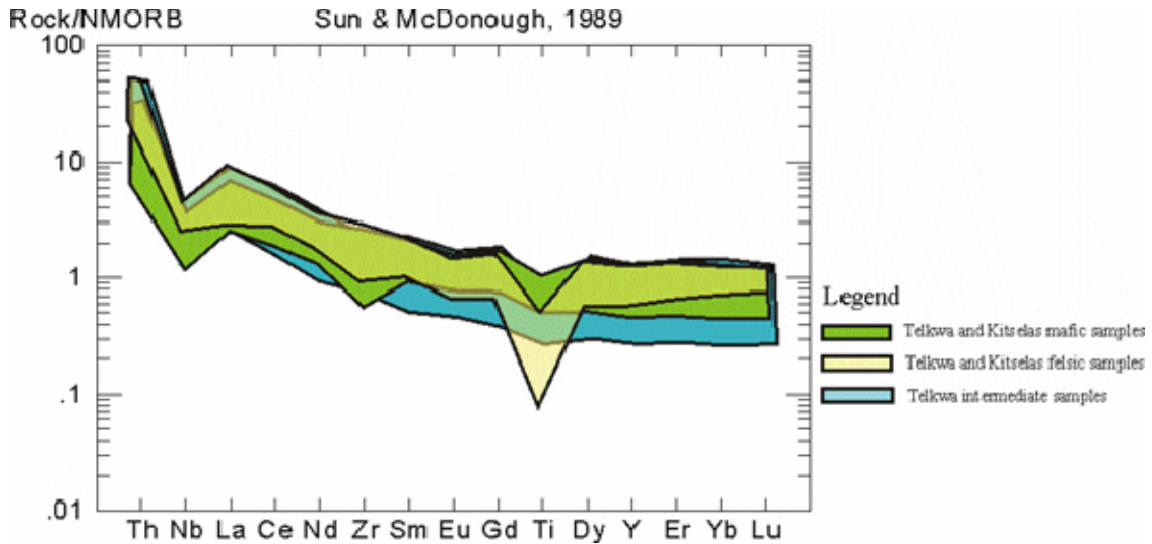


Figure 35: A continuous increase in the concentration of the most incompatible elements and decrease in Ti values implies that felsic samples have been derived from more mafic Telkwa and Kitselas volcanics. Diagram and normalizing values from Sun and McDonough, 1989.

It is worth noting that the intermediate samples tend to occupy the extreme ends of the trace element concentration spectrum. However, one of these samples (05TB-25-3), the one with the lowest concentrations of HFSE, is pyroclastic. This allows for a large amount of variability in its chemistry thus making it far less reliable for geochemical analysis. The other sample (05TB-23-4) shares similar chemical characteristics with the more felsic samples. This is not surprising since it is dacitic in composition and would therefore have been generated later during the evolution of a magma.

#### **(6.4) Normalized Rare Earth Element Diagrams**

##### **(6.4.1) The Rare Earth Elements**

Rare earth elements (REE) are the metals with atomic numbers 57-71 and may also include the element Y. The elements with lower atomic numbers (La, Ce, Pr, Nd, and Pm) are referred to as light rare earth elements (LREE), those with higher atomic

numbers (Tm, Yb, Lu, and Y) are referred to as heavy rare earth elements (HREE), and the middle members (Sm, Er, Gd, Tb, Dy, and Ho) are less commonly referred to as the middle rare earth elements (MREE) (Rollinson, 1993). Differences in their chemical behaviour are derived from a small and steady decrease in ionic size with increasing atomic number (Rollinson, 1993). These differences cause REE's with smaller ionic radii (heavy REE) to be favoured in most solids over a co-existing liquid phase (Winter, 2001). Unlike LFSE, however, REE are generally insoluble and thought to remain immobile during metamorphism and alteration making them very reliable for use in the geochemical analysis of igneous rocks (Rollinson, 1993).

#### **(6.4.2) Interpreting Normalized Rare Earth Element Diagrams**

Normalized REE diagrams are similar to normalized trace element diagrams except that a different reference standard is used; chondritic meteorites are used as the standard in these diagrams as they are thought to represent relatively unfractionated samples of the solar system (Rollinson, 1993).

The degree of fractionation of REE within a system is often expressed as a ratio of the concentration of a lighter REE to that of a heavier REE (in other words by the slope of a REE plot); a  $La/Yb_n$  value of one represents a horizontal line, a value of less than one represents a positive slope, and a value greater than one a negative slope. Likewise, the degree of enrichment or depletion within the HREE or LREE may be expressed by the ratio of the concentration of a middle REE to that of a heavy REE and of the concentration of a light REE to that of a middle REE respectively (Rollinson, 1993).

Enrichment/depletion patterns in REE are similar to those of other trace elements. Normal mid-ocean ridge basalts tend to be depleted in the LREE (the most incompatible of the REE) with respect to chondritic meteorites and thus have average La/Sm ratios of less than one. The depletion in (N)-type MORB reflects their already depleted upper mantle source. Depletion of the upper mantle was likely caused by the extraction of melts to form the primitive oceanic and continental crusts in earlier geologic time (Winter, 2001). Enriched mid-ocean ridge basalts are enriched in the LREE with average La/Sm greater than 1 reflecting their enriched lower mantle source. Both types of mid-ocean ridge basalts tend to have relatively flat HREE patterns (Winter, 2001). Ocean island basalts tend to have similar REE patterns to those of enriched mid-ocean ridge basalts but often have steeper slopes and greater LREE enrichment (Winter, 2001). They also tend to have fractionated HREE patterns indicating that garnet was a residual phase of the system, since it is one of the only common minerals that preferentially incorporates HREE into its structure (Winter, 2001). Lastly, arc basalts tend to have flat HREE patterns and may be depleted or enriched in the LREE depending on the type of arc basalt (Winter, 2001). Low-K (tholeiitic) arc basalts trend to have a positive LREE slope that is flatter than that for an N-MORB. Medium-K or calc-alkaline basalts tend to be slightly enriched in the LREE whereas the high-K basalts are the most enriched of all arc basalts (Winter, 2001). Such variations suggest that arc basalts are generated from more than one source with different LREE concentrations (Winter, 2001).

#### **(6.4.3) Rare Earth Element Patterns in the Telkwa and Kitselas Volcanic Rocks**

Mafic samples from the Telkwa Formation and the Kitselas volcanic sequence show very similar trends in their REE concentrations again suggesting that rocks from

both map units are related (figure 36). La/Sm ratios are between 2.23 and 4.16 indicating that they are enriched in the LREE. HREE trends are relatively flat with Gd/Yb ratios varying between 1.52 and 1.98; values greater than one are representative of the slightly lesser concentrations of the most compatible elements. The Kitselas samples are slightly more enriched in the most compatible elements again possibly implying that they were derived from the melt at a less evolved stage than those from the Telkwa Formation.

Felsic samples from both map units also show very similar trends in their REE concentrations suggesting that they are related (figure 37). La/Sm ratios between 2.34 and 5.05 are representative of a slight enrichment of LREE. HREE trends are relatively flat as Gd/Yb ratios vary between 1.20 and 1.55. Intermediate samples once again plot at the extreme ends of the REE concentration spectrum for the Telkwa Formation and Kitselas volcanic sequence (figure 38). They have La/Sm ratios between 3.81 and 4.35 and Gd/Yb ratios between 1.58 and 1.67. As mentioned above, the sample that occupies the lower end of the concentration spectrum (05TB-25-3) is not as reliable for geochemical analysis because it is volcanoclastic.

An increase in the concentration of LREE (the most incompatible of the REE) from mafic to felsic samples is observed when all of the Telkwa and Kitselas samples are plotted on one Normalized REE diagram (figure 39). This pattern, in conjunction with the similarities in trace element trends between the felsic and mafic samples, suggests that all samples are being derived from the same melt. The overall negative slope within the LREE and relatively flat slope within the HREE further supports the theory that these rocks are part of an island arc suite.

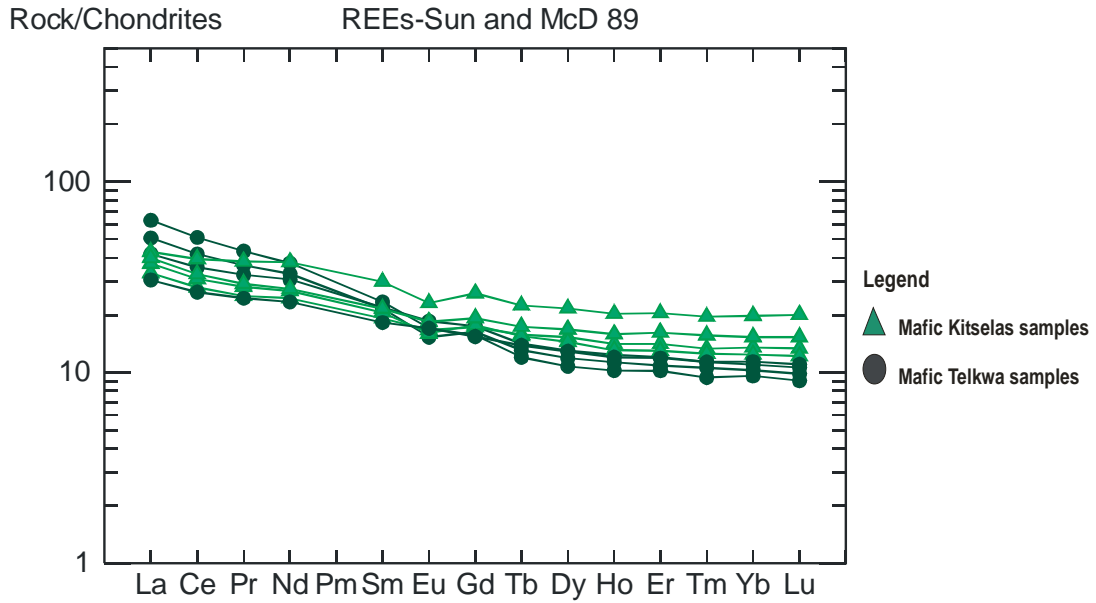


Figure 36: The mafic samples from the Telkwa Formation and the Kitselas volcanic sequence have very similar rare earth element trends. The higher concentration of the more compatible elements in the Kitselas samples may imply that these volcanics have formed slightly earlier than Telkwa samples. Diagram and normalizing values from Sun and McDonough, 1989.

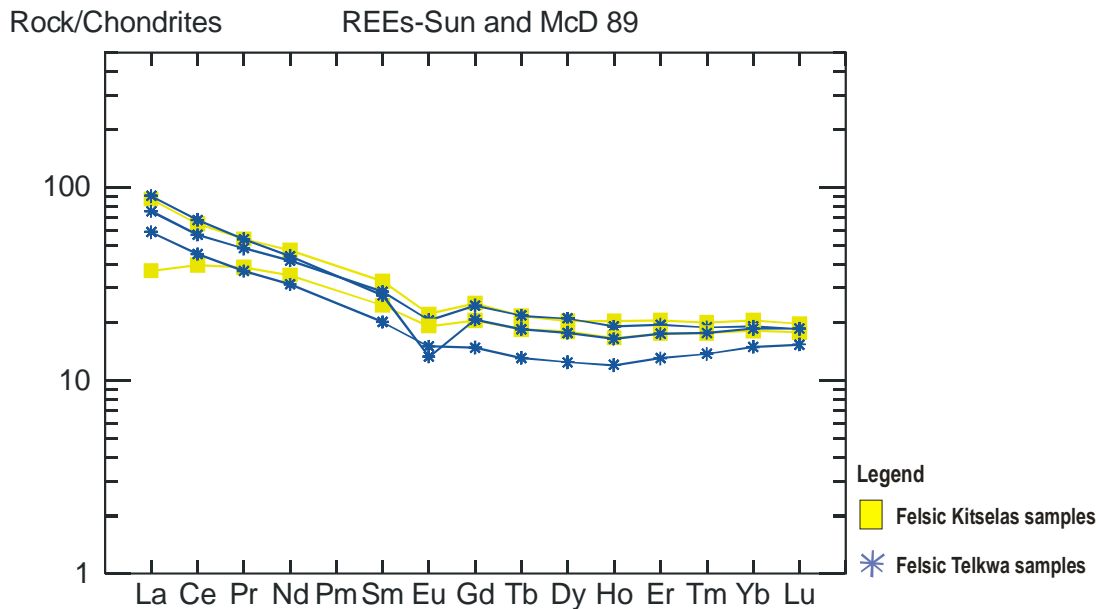


Figure 37: Rare earth element trends for felsic rocks of the Telkwa Formation and the Kitselas volcanic sequence parallel one another suggesting they are related. Diagram and normalizing values from Sun and McDonough, 1989.

### **(6.5) A Comparison of the Field and Petrographic Characteristics of Felsic Rocks from the Kitselas Volcanic Sequence and Telkwa Formation**

Felsic rocks from the Telkwa Formation and Kitselas volcanic sequence have many comparable petrographic features; they share very similar compositions and textures, as they are both massive and flow banded and predominantly composed of potassium feldspar, quartz, and +/- minor plagioclase with minor sericitization. Such characteristics however are typical of most rhyolites.

The felsic rocks comprising the majority of the Kitselas volcanic sequence and felsic rocks of the Telkwa Formation share many of the same field characteristics; both are composed of lapilli tuffs with lesser welded tuffs, ash and crystal ash tuffs, resedimented volcanic rocks, and flow banded layers. However, there are some major differences between Kitselas and Telkwa rocks. The most obvious difference is that the felsic rocks of the Kitselas volcanic sequence are present in unusually large volumes whereas those in the Telkwa Formation form much smaller masses. Secondly, although both share many of the same facies and textures, there are differences in the amounts in which they occur. Exposed Kitselas volcanic rocks are almost entirely composed of lapilli tuffs whereas pyroclastic and sedimentary volcanic rocks are both well represented in the Telkwa Formation. There is also a difference in the composition of lapilli in the Telkwa Formation and Kitselas volcanic sequence; pyroclastic Telkwa beds are often poly lithic whereas those in the Kitselas are often of a single lithology. Lastly, the base of the Kitselas volcanic sequence is comprised of a thick massive felsic section; felsic massive volcanic rocks are found in the Telkwa Formation, however, they are present in much smaller amounts.

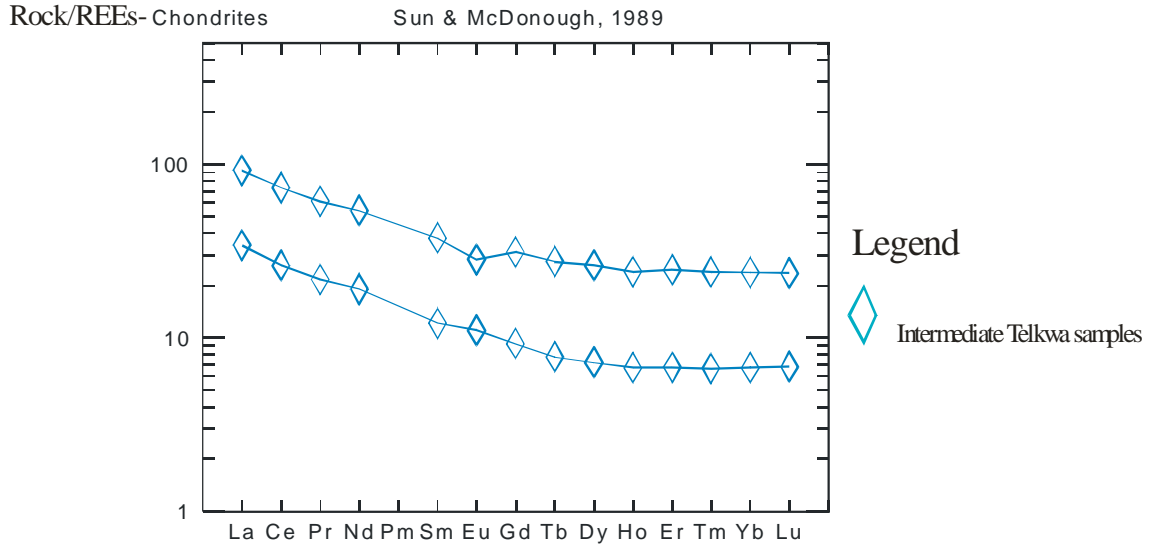


Figure 38: Intermediate samples from the Telkwa Formation define a subduction-related trend. Diagram and normalizing values from Sun and McDonough, 1989.

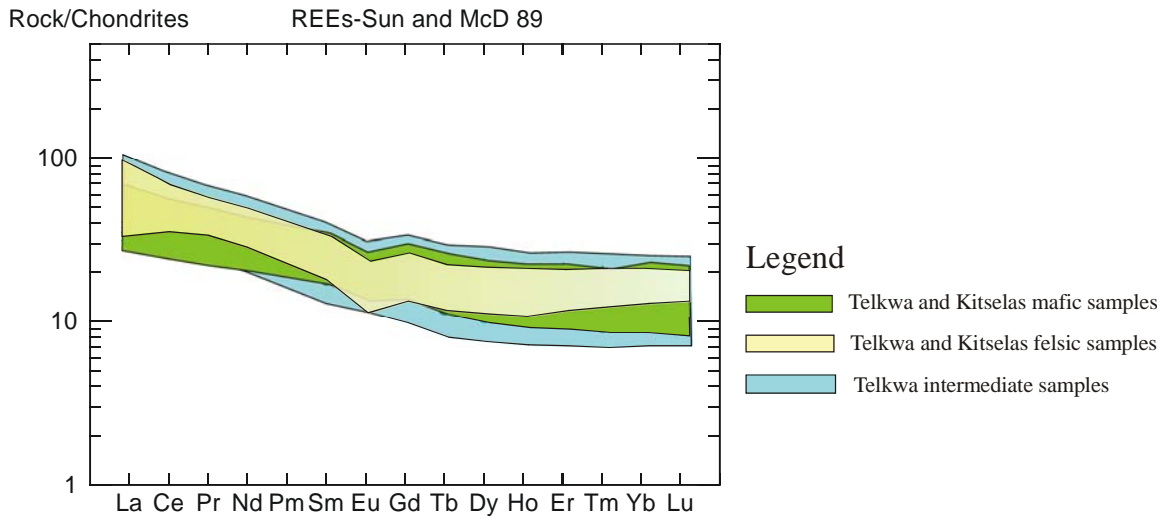


Figure 39: REE patterns for both the felsic and mafic samples overlap; this pattern along with a continuous increase in the concentration of the least compatible elements from mafic to felsic rocks suggests that all of these samples have evolved from a single magma. Diagram and normalizing values from Sun and McDonough, 1989.

Possible explanations for these differences are as follows. The unusual size of the Kitselas body suggests that the Kitselas volcanic rocks are the result of one very massive volcanic event whereas those of the Telkwa were likely the result of many smaller

volcanic events. Although silicic bodies of this size are highly uncommon, silicic tuffs of comparable thickness have been noted elsewhere in the Canadian Cordillera. The most notorious occurrence is that in the Toodoggone area where thick accumulations of white to greenish-grey silicic tuffs subdivide the Sustut Group into the lower Tango Creek Formation and the upper Brother's Peak Formation (Eisbacher, 1971). There are no known analogs for the Kitselas volcanic sequence elsewhere in the Telkwa Formation, however, acidic volcanics of the Howson subaerial facies reach up to 300m in thickness and appear to share many of the same facies and textures with felsic rocks of the Kitselas volcanic sequence; these volcanic rocks are characterized by flow-banded layers, spherulitic flows, welded and non-welded tuffs, vitric-crystal and vitric-crystal-lithic tuffs, breccias, and thick beds of ignimbrites (Tipper and Richards, 1976).

Felsic eruptions tend to be more violent than mafic eruptions due to the high viscosity of silicic magmas leading to the deposition of much larger amounts of pyroclastics. The copious amounts of pyroclastic rocks on Kitselas Mountain are therefore likely the expression of not just a massive volcanic event, but also a very violent one. The homogeneity of pyroclastic components in the Kitselas volcanic sequence may reflect either homogeneity in their source or higher degrees of metamorphism and alteration; the latter of the two possibilities may have masked various features originally present in the Kitselas volcanic rocks.

The higher quantity of resedimented material in the Telkwa indicates that these volcanic rocks were deposited in environments subjected to more sedimentary processes as compared to the depositional environments of the Kitselas volcanic sequence. As for the massive section, it has been postulated that the felsic Telkwa rocks probably represent

the flanks of larger unexposed rhyolite bodies (Barresi and Nelson, 2005). If this were the case, it is likely that the more massive rhyolitic/dacitic rocks lie closer to an edifice that has since been eroded or is simply unexposed. It is likely that the pyroclastic rocks of the Kitselas volcanic sequence also represent the flanks of an edifice whereas the massive section would represent proximity to a volcanic centre and possibly a dome or dome-flow complex (Winter, 2001). Further supporting this suggestion is the fact that the resedimented unit on Kitselas Mountain shows evidence of being deposited in a subaqueous depositional environment. This resedimented unit lies far to the west of the massive body and thus would represent a more distal location from the edifice, which in turn suggests a lower lying area.

#### **(6.6) A Comparison of the Field and Petrographic Characteristics of Mafic Rocks in the Kitselas Volcanic Sequence and Telkwa Formation:**

Although the more mafic samples of the Telkwa Formation and Kitselas volcanic sequence have very similar primary mineralogies, there are quite a few variations in their alteration and textural patterns both in micro and outcrop scale. More specifically, the mafic samples taken from Kitselas Mountain share very similar textures and tend to be altered to greenschist metamorphic facies, whereas those from the Telkwa Formation have many different textures and have undergone several different types of alteration. Possible explanations for these variations are as follows. Firstly, the fact that greenschist metamorphic mineral assemblages are found in most of the Kitselas samples and are only found in a few of the Telkwa samples can be explained by the hypothesis that the Kitselas volcanic rocks comprise the foot wall of a detachment fault system. If this is the case, the Kitselas volcanic rocks would have been subjected to higher pressure and temperature

conditions prior to their exhumation; the lower stratigraphic position of the Kitselas volcanic sequence could have easily led to the development of greenschist metamorphic grade. The orientation of deformational fabrics on Kitselas Mountain, the slightly higher concentration of compatible elements, and the fault contact between Kitselas and Telkwa rocks supports this theory. The appearance of actinolite in Telkwa samples could be explained by a transitional contact between greenschist and zeolite metamorphic grades. In this case, some rocks found lower in the stratigraphy of the Telkwa Formation may have experienced similar pressure and temperature conditions to those experienced by rocks of the Kitselas volcanic sequence.

The simplest and most probable explanation for the overall variety of textures and alteration patterns within the mafic Telkwa rocks as compared to those in the mafic Kitselas rocks involves the thicknesses of these map units. Mafic Telkwa rocks represent about a third of the Usk map sheet while those from Kitselas Mountain only occur as three thin flows of about 60 to 250m in thickness. Therefore, the probability of there being a greater variety of textures and alteration patterns in the Telkwa Formation is quite high.

#### **(6.7) Sources of Error**

The most likely source of error in this project is the sample size, as only a small part of the population was analyzed. Generally speaking, the smaller the sample size, the greater the uncertainty in the results. It was especially difficult to attain a representative number of Kitselas samples, as most of the sequence is composed of volcanoclastic rocks.

**(7.0) Summary and Conclusion:**

The Kitselas volcanic sequence lies within the western portion of the Usk map area. Gareau et al. (1997) previously determined that rocks of the Kitselas volcanic sequence are coeval in age with rocks of the Telkwa Formation; however, the primary relationship between the two rock packages was unclear due to differences in composition, metamorphic grade, and deformational features. The purpose of this thesis was to describe the Kitselas volcanic rocks in terms of volcanology, petrography, and geochemistry and to use this data to determine the primary relationship between the Kitselas volcanic rocks and rocks of the Telkwa Formation.

Major and trace element chemistry indicate that Telkwa and Kitselas rocks are part of an island arc calc-alkaline suite. Similarities in trace and REE patterns between the two units indicate that they are likely related. A continuous increase in the concentration of the most incompatible elements accompanied by a decrease in Ti concentrations from mafic to felsic samples suggest that felsic Telkwa and Kitselas rocks have been derived from the evolution of a magma rather than by crustal melting. Higher concentrations of the most compatible trace and rare earth elements in the Kitselas samples suggests that the Kitselas volcanic rocks may have begun to form prior to the development of the Telkwa volcanic rocks.

Petrographic analysis of the Telkwa and Kitselas samples revealed important similarities and differences between the two rock packages. Felsic Telkwa and Kitselas rocks share very similar compositions and textures supporting the suggestion that these rocks are related. Mafic Telkwa and Kitselas rocks share very similar primary mineralogies supporting this theory; however, there are differences in their textures and

alteration patterns. These variations could easily be due to the different thicknesses and extent of the two map units; it is likely that volcanic rocks of the Telkwa Formation would develop a greater number of textures and alteration patterns because they are present in such large volumes. The greenschist metamorphic mineral assemblage observed in the mafic Kitselas samples supports the suggestion that these volcanic rocks were originally, or at least at one time, positioned below the Telkwa Formation. The presence of the Usk fault further supports this suggestion.

The large size of the Kitselas volcanic sequence and the copious amounts of pyroclastic material suggests that this section is the result of a very massive and violent volcanic event. The homogeneity of the pyroclastic components may reflect either homogeneity in the source material or higher degrees of alteration and metamorphism. Massive material at the base of the exposed section likely represents proximity to a volcanic centre, whereas lower lying parts of the edifice flanks are represented in the west by a sub-aqueous volcanic conglomerate unit.

Appendix

Table A-1: Major and Trace Element Data Determined by X-ray Fluorescence Spectrometry at the Saint Mary's Geochemical Center.

| SAMPLE    | L.O.I.<br>% | SiO2<br>% | TiO2<br>% | Al2O3<br>% | Fe2O3<br>% | MnO<br>% | MgO<br>% | CaO<br>% | Na2O<br>% | K2O<br>% | P2O5<br>% | V<br>ppm | Cr<br>ppm | Co<br>ppm | Zr<br>ppm | Ba<br>ppm |
|-----------|-------------|-----------|-----------|------------|------------|----------|----------|----------|-----------|----------|-----------|----------|-----------|-----------|-----------|-----------|
| 05NB-01-1 | 6.06        | 51.66     | 0.860     | 15.95      | 8.43       | 0.142    | 5.21     | 6.27     | 2.99      | 1.39     | 0.289     | 5        | 91        | 35        | 82        | 503       |
| 05NB-03-6 | 3.29        | 49.17     | 1.078     | 17.66      | 10.02      | 0.155    | 6.98     | 6.53     | 4.26      | 0.12     | 0.265     | 247      | 191       | 54        | 70        | 88        |
| 05NB-07-1 | 0.39        | 72.29     | 0.574     | 13.35      | 3.04       | 0.036    | 0.47     | 1.23     | 4.76      | 2.45     | 0.127     | 15       | <5        | 7         | 169       | 405       |
| 05NB-15-5 | 3.04        | 54.21     | 0.781     | 18.46      | 6.55       | 0.198    | 3.06     | 6.50     | 3.83      | 2.41     | 0.317     | 150      | <5        | 23        | 99        | 973       |
| 05NB-23-2 | 0.71        | 74.43     | 0.527     | 12.64      | 4.79       | 0.072    | 0.09     | 0.30     | 5.00      | 2.36     | 0.127     | 32       | 10        | 16        | 163       | 562       |
| 05NB-23-4 | 3.82        | 62.78     | 0.889     | 14.83      | 6.01       | 0.084    | 0.56     | 2.54     | 3.14      | 4.87     | 0.352     | 99       | <5        | 16        | 142       | 1118      |
| 05NB-26-1 | 1.70        | 52.92     | 0.965     | 15.90      | 10.22      | 0.199    | 4.98     | 6.30     | 3.49      | 2.59     | 0.201     | 311      | 40        | 41        | 79        | 890       |
| 05NB-26-3 | 0.20        | 77.81     | 0.300     | 11.24      | 2.27       | 0.019    | <0.01    | 0.15     | 4.52      | 2.81     | 0.063     | 13       | <5        | 6         | 187       | 610       |
| 05NB-28-1 | 4.12        | 54.82     | 1.135     | 16.40      | 7.69       | 0.121    | 2.09     | 3.94     | 6.01      | 2.57     | 0.376     | 196      | <5        | 26        | 134       | 990       |
| 05NB-28-2 | 4.01        | 48.14     | 1.062     | 18.08      | 10.24      | 0.278    | 11.53    | 1.14     | 4.78      | 1.38     | 0.234     | 376      | 36        | 56        | 67        | 623       |
| 05NB-29-2 | 2.36        | 54.18     | 1.092     | 15.92      | 10.83      | 0.393    | 6.18     | 1.37     | 4.83      | 2.15     | 0.221     | 316      | 25        | 53        | 81        | 1329      |
| 05TB-25-3 | 2.18        | 60.09     | 0.464     | 16.47      | 6.18       | 0.12     | 2.97     | 6.52     | 2.55      | 1.8      | 0.133     | 148      | 32        | 23        | 76        | 641       |
| 05TB-31-1 | 2.51        | 49.63     | 1.034     | 17.86      | 10.85      | 0.188    | 5.64     | 8.96     | 2.62      | 0.58     | 0.215     | 305      | 102       | 44        | 54        | 339       |
| 05TB-33-1 | 0.48        | 78.97     | 0.124     | 11.98      | 1.49       | 0.082    | 0.53     | 1.81     | 2.81      | 2.89     | 0.049     | 12       | 11        | <5        | 88        | 1026      |
| 05TB-39-9 | 0.87        | 76.20     | 0.211     | 12.76      | 1.58       | 0.053    | 0.20     | 0.38     | 4.57      | 2.54     | 0.045     | 5        | <5        | <5        | 182       | 749       |

Table A-2: Major and Trace Element Data Determined by X-ray Fluorescence Spectrometry at the Saint Mary's Geochemical Center (continued).

| SAMPLE    | La<br>ppm | Nd<br>ppm | Ni<br>ppm | Cu<br>ppm | Zn<br>ppm | Ga<br>ppm | Rb<br>ppm | Sr<br>ppm | Y<br>ppm | Nb<br>ppm | Pb<br>ppm | Th<br>ppm | U<br>ppm | Totals |
|-----------|-----------|-----------|-----------|-----------|-----------|-----------|-----------|-----------|----------|-----------|-----------|-----------|----------|--------|
| 05NB-01-1 | 26        | 31        | 42        | <4        | 101       | 16        | 39        | 316       | 23       | 2         | 31        | 9         | 2        | 99.25  |
| 05NB-03-6 | 36        | 37        | 76        | 13        | 101       | 18        | 9         | 402       | 21       | 2         | 6         | 5         | 2        | 99.53  |
| 05NB-07-1 | 13        | 18        | <3        | 17        | 32        | 12        | 77        | 199       | 49       | 4         | 33        | 24        | 4        | 98.72  |
| 05NB-15-5 | 21        | 33        | <3        | 30        | 123       | 19        | 45        | 573       | 23       | 1         | 11        | 10        | 2        | 99.36  |
| 05NB-23-2 | 22        | 33        | <3        | 13        | 50        | 12        | 53        | 44        | 47       | 29        | 28        | 21        | 4        | 101.05 |
| 05NB-23-4 | 25        | 40        | <3        | <4        | 247       | 15        | 92        | 76        | 39       | 7         | 29        | 13        | 2        | 99.88  |
| 05NB-26-1 | 23        | 39        | 16        | <4        | 92        | 20        | 47        | 452       | 19       | 1         | 10        | 3         | 1        | 99.47  |
| 05NB-26-3 | 8         | 22        | <3        | 26        | 34        | 9         | 66        | 65        | 55       | 27        | 38        | 27        | 5        | 99.38  |
| 05NB-28-1 | 26        | 44        | <3        | <4        | 163       | 16        | 52        | 161       | 34       | <1        | 18        | 9         | 2        | 99.27  |
| 05NB-28-2 | 40        | 61        | 60        | <4        | 521       | 20        | 38        | 158       | 24       | 4         | 25        | 9         | 3        | 100.87 |
| 05NB-29-2 | 40        | 74        | 8         | 8         | 423       | 21        | 35        | 94        | 23       | <1        | 12        | 5         | 3        | 99.53  |
| 05TB-25-3 | 15        | 21        | 6         | <4        | 86        | 18        | 40        | 378       | 20       | 8         | 16        | 10        | 2        | 99.48  |
| 05TB-31-1 | 27        | 28        | 62        | 135       | 105       | 21        | 12        | 371       | 17       | 1         | <3        | 2         | 1        | 100.09 |
| 05TB-33-1 | 9         | 21        | <3        | 29        | 41        | 11        | 84        | 166       | 50       | 26        | 35        | 28        | 5        | 101.22 |
| 05TB-39-9 | 10        | 23        | <3        | 27        | 32        | 12        | 79        | 100       | 48       | 8         | 42        | 29        | 5        | 99.41  |

Table A-3: Trace Element and REE Data Acquired from Memorial University using Inductively Coupled Mass Spectrometry.

| SAMPLE    | Y ppm | Zr ppm | Nb ppm | La ppm | Ce ppm | Pr ppm | Nd ppm | Sm ppm | Eu ppm | Gd ppm | Tb ppm | Dy ppm | Ho ppm | Er ppm | Tm ppm | Yb ppm | Lu ppm | Hf ppm | Ta ppm | Th ppm |
|-----------|-------|--------|--------|--------|--------|--------|--------|--------|--------|--------|--------|--------|--------|--------|--------|--------|--------|--------|--------|--------|
| 05NB-01-1 | 16.08 | 95.58  | 6.64   | 12.01  | 25.58  | 3.47   | 15.37  | 3.31   | 0.89   | 3.36   | 0.49   | 3.02   | 0.64   | 1.80   | 0.27   | 1.75   | 0.25   | 2.36   | 0.21   | 1.41   |
| 05NB-03-6 | 17.66 | 78.14  | 5.35   | 9.92   | 21.80  | 3.09   | 14.34  | 3.35   | 1.08   | 3.59   | 0.53   | 3.31   | 0.70   | 2.00   | 0.29   | 1.87   | 0.27   | 2.10   | 0.15   | 1.00   |
| 05NB-07-1 | 29.97 | 181.05 | 9.71   | 20.58  | 39.54  | 5.14   | 22.01  | 4.99   | 1.28   | 5.16   | 0.81   | 5.17   | 1.15   | 3.39   | 0.51   | 3.47   | 0.50   | 4.22   | 0.50   | 4.18   |
| 05NB-15-5 | 14.96 | 109.22 | 7.39   | 14.88  | 31.25  | 4.11   | 17.52  | 3.58   | 0.99   | 3.23   | 0.45   | 2.74   | 0.58   | 1.69   | 0.24   | 1.63   | 0.23   | 2.86   | 0.23   | 3.37   |
| 05NB-23-2 | 27.6  | 111.61 | 8.57   | 17.82  | 34.76  | 4.59   | 19.51  | 4.41   | 1.19   | 5.03   | 0.81   | 5.32   | 1.08   | 3.22   | 0.48   | 3.24   | 0.47   | 2.52   | 0.43   | 4.73   |
| 05NB-23-4 | 34.5  | 157.88 | 9.75   | 21.85  | 44.81  | 5.83   | 25.26  | 5.74   | 1.64   | 6.41   | 1.03   | 6.64   | 1.36   | 4.08   | 0.61   | 4.05   | 0.59   | 4.09   | 0.35   | 5.27   |
| 05NB-26-1 | 19.85 | 82.91  | 3.21   | 7.87   | 17.12  | 2.39   | 11.45  | 2.94   | 0.97   | 3.56   | 0.59   | 3.90   | 0.80   | 2.34   | 0.34   | 2.30   | 0.34   | 2.30   | 0.09   | 1.23   |
| 05NB-26-3 | 25.46 | 116.23 | 6.80   | 8.77   | 24.26  | 3.67   | 16.37  | 3.75   | 1.11   | 4.21   | 0.69   | 4.55   | 0.94   | 2.90   | 0.45   | 3.08   | 0.45   | 2.35   | 0.36   | 3.04   |
| 05NB-28-1 | 30.25 | 161.44 | 7.45   | 10.17  | 24.11  | 3.63   | 17.70  | 4.57   | 1.34   | 5.34   | 0.84   | 5.51   | 1.15   | 3.39   | 0.50   | 3.37   | 0.51   | 4.17   | 0.24   | 3.02   |
| 05NB-28-2 | 18.42 | 76.10  | 3.83   | 8.83   | 18.93  | 2.67   | 12.49  | 3.16   | 0.93   | 3.64   | 0.58   | 3.68   | 0.74   | 2.15   | 0.32   | 2.11   | 0.31   | 2.00   | 0.13   | 0.90   |
| 05NB-29-2 | 22.64 | 96.86  | 3.82   | 9.44   | 20.06  | 2.77   | 12.82  | 3.31   | 1.07   | 3.96   | 0.65   | 4.27   | 0.90   | 2.68   | 0.40   | 2.61   | 0.39   | 2.52   | 0.09   | 1.46   |
| 05TB-25-3 | 9.94  | 76.99  | 4.58   | 8.10   | 16.01  | 2.06   | 8.93   | 1.86   | 0.64   | 1.90   | 0.29   | 1.83   | 0.38   | 1.12   | 0.17   | 1.14   | 0.17   | 2.15   | 0.17   | 1.35   |
| 05TB-31-1 | 17.1  | 48.80  | 3.25   | 7.24   | 16.15  | 2.33   | 10.95  | 2.80   | 0.99   | 3.17   | 0.52   | 3.28   | 0.68   | 1.97   | 0.29   | 1.94   | 0.28   | 1.42   | 0.09   | 0.87   |
| 05TB-33-1 | 25.76 | 78.33  | 8.54   | 21.38  | 41.54  | 5.12   | 20.56  | 4.23   | 0.77   | 4.25   | 0.69   | 4.48   | 0.93   | 2.89   | 0.45   | 3.15   | 0.47   | 2.78   | 0.44   | 5.34   |
| 05TB-39-9 | 18.54 | 158.33 | 6.91   | 13.89  | 27.60  | 3.50   | 14.70  | 3.07   | 0.87   | 3.04   | 0.49   | 3.16   | 0.68   | 2.16   | 0.35   | 2.54   | 0.39   | 3.34   | 0.36   | 3.20   |

## Acknowledgements

I would first like to thank my family, especially my mother and father, for their never-ending support, without which my work and success would not have been possible. Thanks to Dr. Jarda Dostal who recognized my potential and guided me through so many once in a lifetime opportunities. There are no words to describe my appreciation for your friendship.

To JoAnne Nelson of the Geological Survey of British Columbia for taking me under her wing and opening my eyes to a whole new world. Your extraordinary leadership, kindness, and patience have led me to become not just a better geologist, but also a better person.

I would like to thank Tony Barresi, who is not only my very good friend, but also one of my mentors. Thank you for your encouragement, the knowledge you have passed down to me, and for showing me how to teach myself.

I extend my thanks to Brian Grant of the Geological Survey of British Columbia for his guidance, encouragement, and support. Thank you for never failing to answer a question. Thank you to the faculty and staff of the Saint Mary's Geology Department for everything you have done for me over the past three long years.

Last, but definitely not least, I am forever grateful to my very close friends who have stood by me from the very beginning; I hope you will all be there to the end.

## References

- Anderson, R.G., 1989. A Stratigraphic, Plutonic, and Structural Framework for the Iskut River Map Area, NW British Columbia. In: Current Research, Part E, Geological Survey of Canada, paper 89-1E. pages 145-154.
- Bagnold, R. A., 1954. Experiments on a Gravity-Free Dispersion of Large Solid Spheres in a Newtonian Fluid under Shear. Proceedings of the Royal Society, London, A225, 49-63.
- Bailes, A. H., Christiansen, E. H., Galley, A. G., Jenner, G. A., Keith, J. D., Kerrich, R., Lentz, D. R., Leshner, C. M., Lucas, S. B., Ludden, J. N., Pearce, J. A., Peloquin, S. A., Stern, R. A., Stone, W. E., Syme, E. C., Swinden, H. S., and Wyman, D. A., 1996. Trace Element Geochemistry of Volcanic Rocks: Applications for Massive Sulphide Exploration. Geological Association of Canada.
- Barresi, T., Nelson, J. L., 2006. Usk Map Area (NTS 103I/09), Near Terrace, British Columbia: Cross-Sections and Volcanic Facies Interpretation. Geological Fieldwork 2005, Paper 2005-4, pages 21 – 28.
- Branney, M. J., Kokelaar, P., 2002. Pyroclastic Density Currents and the Sedimentation of Ignimbrites. The Geological Society of London.

- Carter, N. C., 1970. Gold Star. In: *Geology, Exploration, and Mining in British Columbia 1970*. BC Ministry of Energy, Mines, and Petroleum Resources. pages 195 – 197.
- DePAOLO, J.D., 1980. Trace Element and Isotopic Effects of Combined Wallrock Assimilation and Fractional Crystallization. *Earth and Planetary Letters*, vol. 53, pages 189 – 203.
- Eisbacher, G.H., 1971. A Subdivision of the Upper Cretaceous-Lower Tertiary Sustut Group, Toodoggone Map-Area, British Columbia. *Geological Survey of Canada, Paper 70-68*, 16p.
- Gabrielse, H., Yorath, C. J., 1992. *Geology of the Cordilleran Orogen in Canada*. Geological Survey of Canada.
- Gareau, S.A., Friedman, R.M., Woodsworth, G.J., Childe, F., 1997. U-Pb Ages from the Northeastern Quadrant of Terrace Map Area, West-Central British Columbia. In: *Current Research 1997-A, Cordillera and Pacific Margin*. Natural Resources Canada. pages 31 – 40.
- Gareau, S. A., Woodsworth, G.J., Rickli, M., 1977. Regional Geology of the Northeastern Quadrant of Terrace Map Area, West-central British Columbia. In: *Current Research 1997-A, Cordillera and Pacific Margin*. Natural Resources Canada. pages 47 – 55.
- Gregoire, M., McInnes, B.I.A., O'Reilly, S.Y., 2001. Hydrous Metasomatism of Oceanic Sub-Arc Mantle, Lihir, Papua New Guinea, Part 2. Trace Element Characteristics of Slab-Derived Fluids. *Lithos*, vol. 59, pages 91 – 108.
- Leyrit, H., Montenat, C., 2000. *Volcaniclastic Rocks from Magmas to Sediments*. Gordon and Breach Science Publishers.
- Mardson, H., Thorkelson, D.J., 1992. Geology of the Hazelton Volcanic Belt in British Columbia: Implications for the Early to Middle Jurassic Evolution of Stikinia. *Tectonics*. vol. 11, no 6, pages 1266-1287
- McPhie, J., Doyle, M., Allen, R., 1993. *Volcanic Textures*. CODES.
- Miyashiro, A., 1974. Volcanic Rock Series in Island Arcs and Active Continental Margins. *American Journal of Science*, vol. 274, pages 321 – 355.
- Moore, E. M., Twiss, R. J., 1995. *Tectonics*. W. H. Freeman and Company.

- Natural Resources Canada; Geological Survey of Canada. (2006, September). Cordilleran Geoscience, The Five Belt Framework of the Canadian Cordillera. Retrieved November 30, 2006, from [http://gsc.nrcan.gc.ca/cordgeo/belts\\_e.php](http://gsc.nrcan.gc.ca/cordgeo/belts_e.php)
- Natural Resources Canada; Geological Survey of Canada. (2006, September). Cordilleran Geoscience, Pieces of a Giant Jigsaw Puzzle: Cordilleran Terranes. Retrieved November 30, 2006, from [http://gsc.nrcan.gc.ca/cordgeo/terrane\\_e.php](http://gsc.nrcan.gc.ca/cordgeo/terrane_e.php)
- Nelson, J. L., Barresi, T., Knight, E., Boudreau, N., 2006. Geology and Mineral Potential of the Usk Map Area (103I/09) Near Terrace, British Columbia. Geological Fieldwork 2005, Paper 2006-1, pages 117 – 135.
- Pearce, J.A., Cann, J.R., 1973. Tectonic Setting of Basic Volcanic Rocks Determined Using Trace Element Analysis. *Earth and Planetary Science Letters*, vol. 19, pages 290 – 300.
- Ringwood, A.E., 1990. Slab-Mantle Interactions, Petrogenesis of Intraplate Magmas and Structure of the Upper Mantle. *Chemical Geology*, vol. 82, pages 187 – 207.
- Rollinson, H., 1993. *Using Geochemical Data*, J.Wiley and Sons.
- Tipper, H.W., Richards, T.A., 1976. Jurassic Stratigraphy and History of North-Central British Columbia. Geological Survey of Canada.
- Winchester, J.A., Floyd, P.A., 1975. Geochemical Magma Type Discrimination: Applications to Altered and Metamorphosed Basic Igneous Rocks. *Earth and Planetary Letters*, vol. 28, pages 459 – 469.
- Winchester, J.A., Floyd, P.A., 1976. Geochemical Discrimination of Different Magma Series and their Differentiation Products Using Immobile Elements. *Chemical Geology*, vol. 20, pages 325 – 343.
- Winter, J. D., 2001. *An Introduction to Igneous and Metamorphic Petrology*. Prentice Hall Inc.